10-1-1974

The influence of the technologist, image size and image density on the visual measurement of the size of microimages

Walter Shafer

THE INFLUENCE OF THE TECHNOLOGIST, IMAGE SIZE AND IMAGE DENSITY ON THE VISUAL MEASUREMENT OF THE SIZE OF MICROIMAGES

by

Walter F. Shafer

A thesis submitted in partial fulfillment of the requirements for the degree of Master of Science in the School of Photography in the College of Graphic Arts and Photography of the Rochester Institute of Technology

October, 1974

Thesis advisor: Professor Hollis N. Todd

TABLE OF CONTENTS

LIST OF TABLES

LIST OF FIGURES

INTRODUCTION

Brief Overview

Photogrammetry is defined as "the science or art of obtaining reliable measurements by means of photography".[1] The photograph is a two-dimensional reproduction of the three dimensional scene in the field of view of the camera. With prior knowledge about the geometry of the camera and about the geometry of the scene relative to the camera, the photogrammetrist can measure the dimension of an image and subsequently compute the size of the corresponding object in the scene. An oversimplified example is the formula for magnification of a distant object:

$$\text{Size of Object} = \frac{\text{Distance from Camera to Object}}{\text{Camera Focal Length}} \times \text{Size of Image}$$

In the case of aerial photography, precise mathematical models can be generated to simulate the optics and operation of the camera. The position and pointing of the camera can also be determined so that a measurement in the image can result in a calculation of a ground dimension with less than a few percent error. These basic

---

[1] Thompson, M. M., editor. Manual of Photogrammetry (Falls Church, Va.: American Society of Photogrammetry, 1966) p. 1.

geometrical principles of the art of Photogrammetry are derived many times in the literature and have proven accurate for images in the macro scale. (Macro in this case refers to images on the order of one millimeter or larger in size). As images get smaller and smaller on the micro scale, not only is the geometry of the imaging system significant, but now the spread function of the image is significant relative to the overall size of the image. When a technologist takes a measurement on the film, the apparent edge as represented by the image will not be where the true edge is located. At the present state of the art, a systematic method does not exist for precisely predicting what the spread of the microimage will be in an aerial photograph.

The following major factors, among others, contribute to the spread of a microimage in an aerial photograph:

atmosphere
optics of camera
emulsion of original negative
printer
chemical process of negative and duplicate
emulsion of duplicate film

In addition, the measurement of the microimage is influenced by the type of equipment used to make the measurement and the technologist who visually selects the edges of the image to be measured.

With the advent of high quality optics and film capable of producing images of fine detail (over 150 cycles/millimeter in some cases), a need exists for the

investigation of the factors influencing the measurement of microimages. The experiment described in this paper was conducted to investigate three factors which may influence the visual measurement of a microimage in a photograph. The first factor was the technologist performing the task. The experiment was intended to determine if there is a significant difference among technologists in selecting the edge of a microimage and the results demonstrate where their prediction falls relative to a microdensitometer scan of the image and how it relates to the actual image size. This part of the experiment gives a graphical indication as to whether a mechanical measurement such as that produced by a microdensitometer might be more reliable than a visual measurement.

The second factor was the image width as recorded on the positive film. The experiment was intended to determine the relationship between the measured image width and the error or "measured imaged width minus actual image width". Image widths of rectangular objects ranging from ten to 300 micrometers, all recorded at the same density, were investigated.

The third factor was density of the image. Because the spread of an image increases with increasing exposure, a functional relationship has been examined between the density of the image and the measurement error.

This experiment did not investigate the influence of the printing process, the original negative, the camera optics, or the atmosphere as they affect an aerial image. The problem is complex and must be attacked one factor at a time. The remaining factors could be incorporated into later experiments. This one experiment resulted in the calibration of one film and one measurement technique. There is no reason to believe, however, that the methods and procedures developed in this experiment cannot be employed to investigate other factors.

Theoretical Background: Basic Theory

The investigations in this experiment were concerned with the widening of an image in a photographic film, the reduction of edge sharpness, and the effect of these two factors on the visual determination of the size of the image.

We will omit for the immediate discussion the visual aspect of edge selection and examine the physical situation on the film. If a knife edge in contact with a film is image on the film, the theoretical light distribution as it reaches the emulsion will appear as shown in Figure 1, ignoring diffraction at the knife edge. Some density will be formed in the area shielded by the knife edge, the amount of density depending on the intensity of light and type of film. This is due to light energy reaching this area within the emulsion by reason of

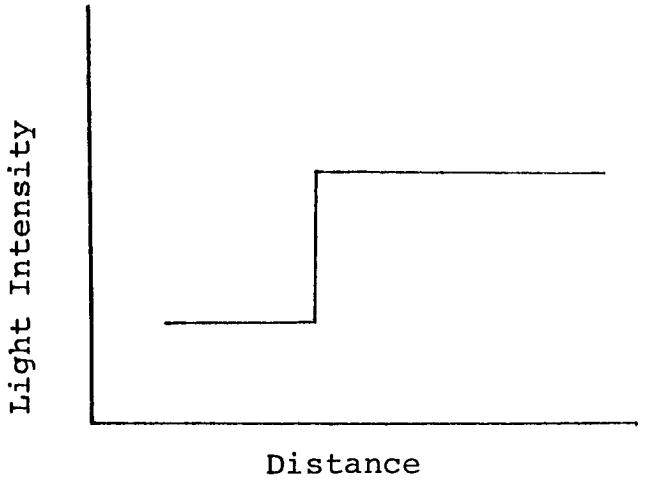

FIGURE 1. Theoretical Light Distribution From a Knife Edge as it Reaches the Emulsion

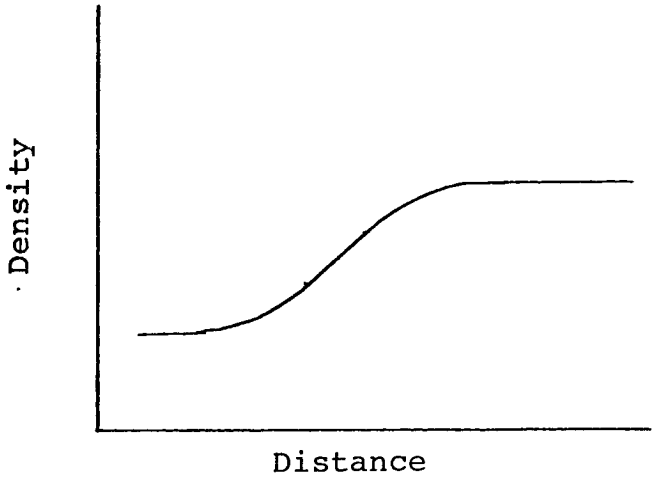

FIGURE 2. Density Trace of a Resultant Image of the Knife Edge

reflection, diffraction, and scattering at the silver halide grains. A density trace of the resultant image of the knife edge on the film would appear as shown in Figure 2.

The property of a material by which light is diffused into the region receiving no direct illumination is optical turbidity. Since the turbidity of an emulsion is normally measured in terms of the diffusion of the image, it should be noted that the photographic turbidity may differ appreciably from optical turbidity.[2] The optical turbidity (refraction, etc.) could be high but if the light diffused sideways is rapidly absorbed, the image is kept in narrow bounds. In the remainder of this experiment, turbidity will refer to photographic turbidity, that is, the diffusion of the image.

The widening of the edge in the image can be expressed in the more recent terminology of the spread function. In Figure 3 is shown a knife edge which separates a uniformly illuminated field A from a dark field B. The illuminated field can be divided into narrow lines parallel to the knife edge. These lines, after passing through the lens and forming an image, provide their own elementary spread

---

[2]James, T. H. and Higgins, G. C. Fundamentals of Photographic Theory (Hastings on Hudson, N.Y.: Morgan and Morgan Inc., 1968) p. 280.

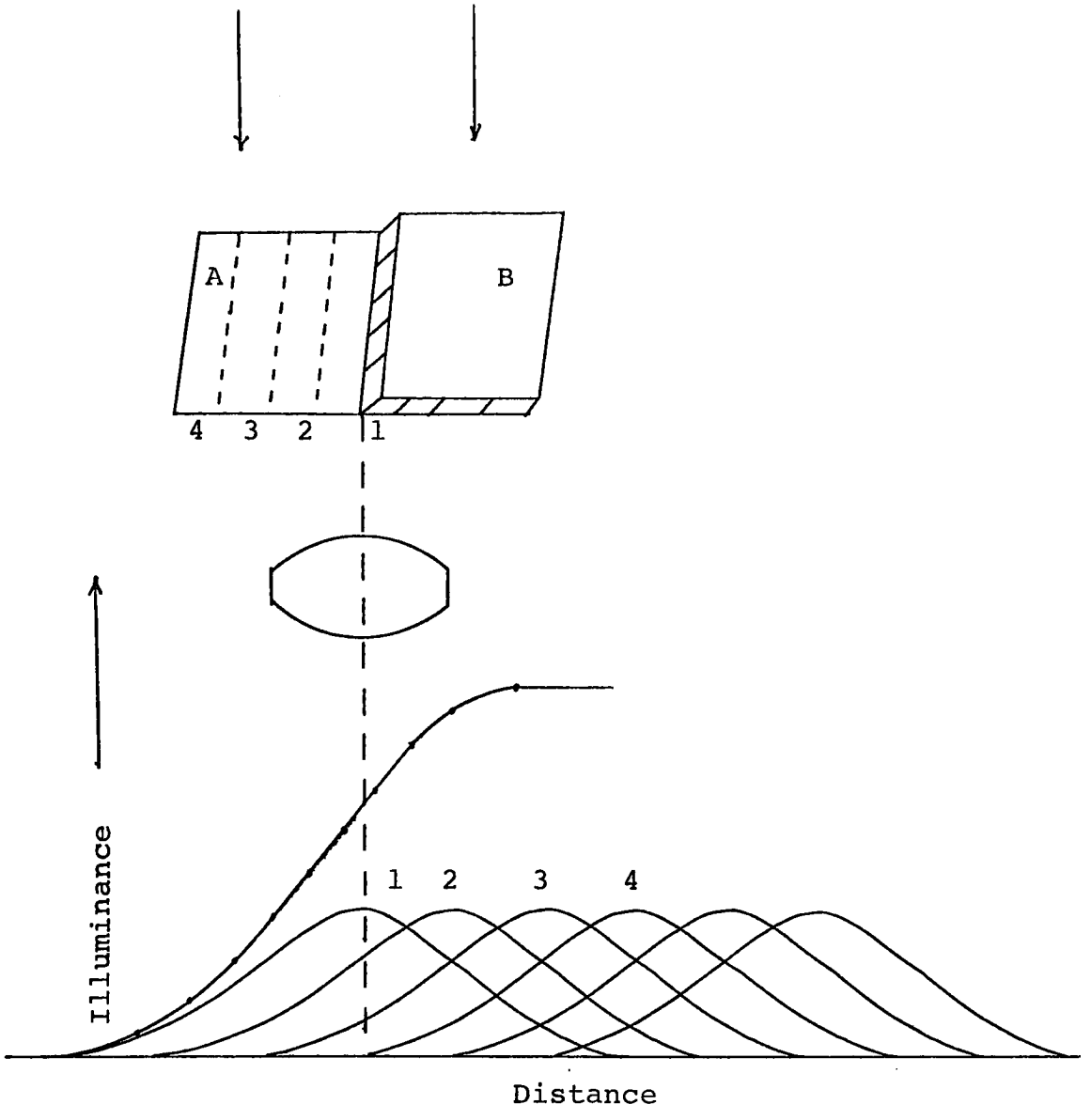

FIGURE 3. Schematic Diagram of Formation of Edge Trace as Summation of Elementary Line Spread Functions

functions (1, 2, 3, 4). The illuminance at any point along the edge is the sum of the ordinates of the elementary spread functions at that point.[3]

A situation similar to the knife edge phenomenon would exist when a slit bounded by a knife edge on each side is imaged onto a film. Each edge of the slit would now be subjected to a similar spread function. The result is shown in the microdensitometer trace of Figure 4.

Now that a brief review of the physical situation on the film has been accomplished, the subject of the visual selection of an edge must be examined. W. N. Charman investigated in 1963 the visual factors in size measurement in microscopy.[4] Charman's experiments involved the measurement through a microscope of an optical image (not film image) of an object. He found three factors in the visual process affected the "visual" size of the image:

(1) retinal illumination,
(2) the magnification of the optics,
(3) the pre-adaptation of the eye.

With proper care, each of these three factors can be optimized so that their influence on a measurement is minimized.

---

[3]Mees, C. E. K. and James, T. H. The Theory of the Photographic Process, 3rd Edition. (New York: The Macmllan Co., 1966). p. 502.

[4]Charman, W. N. Optica Acta. Vol. 10 (1963). p. 129.

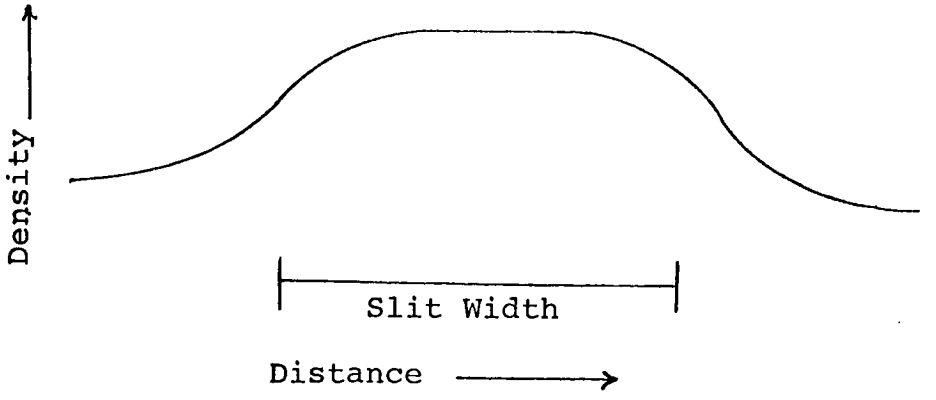

FIGURE 4. Microdensitometer Scan of a Slit Image

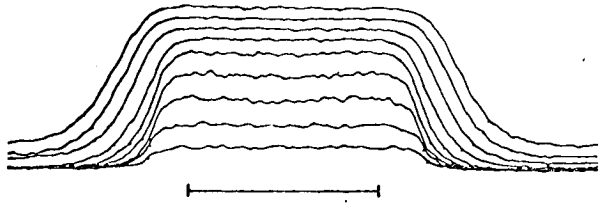

FIGURE 5. Microdensitometer Traces of a Series of Slit Images on a High-Speed Negative Film. [The geometrical width of the slit is shown by the horizontal line. The ticks show the settings by one observer of a filar micrometer on the apparent edge (from Mees and James, p. 508).]

A short investigation was reported in The Theory of the Photographic Process[5] where one observer was used to determine the width of an image. His results are shown in Figure 5.

Theoretical Background: Experimental Design Consideration

Two basically different systems are available for projecting small scale images with sharp edges onto film. The first is to place over the film a glass with an opaque substance on one side. In the opaque layer are etched fine lines with sharp edges. These fine lines are contact printed onto the film. One objection to this method of imaging is that the edges of the lines cause diffraction of the light and would contribute to the spread of the image. In this experiment, it would be desirable to separate the effects of the printing process so that the film effects could be isolated and measured. For this reason, the contact plate method was rejected.

The second system for imaging microimages is by the use of a microcamera. The microcamera is basically a microscope used in reverse and is the principal instrument in the field of Microphotography--a process for making minute, precision photographs of an object.[6] The

---

[5]Mees and James, p. 508.

[6]Eastman Kodak Company. Techniques of Microphotography (Rochester, N.Y., 1967) p. 4.

microcamera has been used in this experiment as the means of projecting images onto the film.

EXPERIMENTAL PROCEDURE

Short Review and Objectives

The images measured in this experiment were bars. The response variable of the experiment was measurement error (measured image width minus the aerial image width). Four bar image widths ranging from seven to three hundred micrometers were used in the experiment. Each of the four bars was imaged at four different densities, ranging from 0.40 to 2.00 (dark bar on a background density at base plus fog), resulting in a total of 16 images. The widths of each of the sixteen images were measured by five experienced photogrammetrists. Using this type of experimental design, a statistical analysis of variance was conducted to fulfill the following objectives:

1. a) To determine if there is a significant difference in measurement error (measured image width minus actual image width) of microimages of rectangular objects when different observers are used for the measurement. b) To determine if there is a significant difference in measurement error of microimages of rectangular objects when different image

widths are used in the measurement. c) To calibrate a given photographic system with respect to the actual image width, the microdensitometer scan of the image, and the visually measured width of the image.

2. To find whether or not there is a relationship between the measured width of the image and the measurement error for a constant density of image and background.

3. To determine for one actual width whether or not there is a relationship between density difference of the image and measurement error (Background density held constant).

Image Exposure

The film selected for this experiment was Eastman Kodak Fine Grain Aerial Duplicating (Type 2430). This is a frequently used aerial duplicating film and will provide for the widest application of results.

The bars were imaged onto the film using a micro-camera (see Figure 6). The microscope consisted of a 10X eyepiece and 8X objective, .32 numerical aperture. The light source was fluorescent with an opal glass cover. Focus control was by Electro Check Sensor Model 230F121

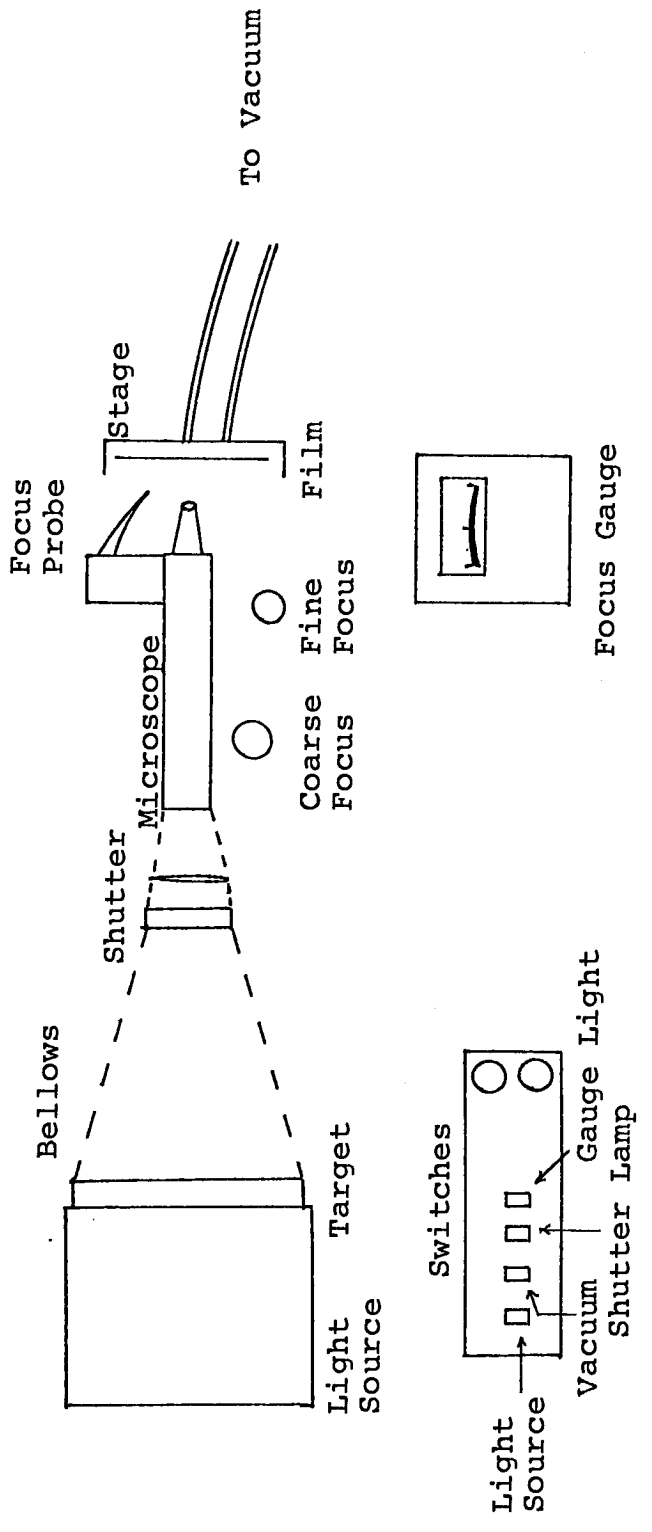

FIGURE 6. Microcamera Apparatus for Exposing Images

by FEDERAL. The Film was held to the platen by a vacuum system from Central Scientific Company, serial number 46805. Four individual bar targets were constructed using black vinyl tape on clear acetate. The bars on the target were of clear acetate with the surrounding area opaque due to the black vinyl tape. The widths of the bar targets were approximately 0.8, 4.0, 8.0, and 24.0 millimeters. Therefore, after an 80 times reduction in the microcamera, the images on film were approximately 10, 50, 100, and 300 micrometers, the range of image widths selected to satisfy the original objectives.

Each target was exposed in the microcamera at various shutter speeds to obtain the four required density levels. Because of inaccuracies in the shutter speed several exposures had to be made to achieve the four precise density levels required for each of the targets. Target 1 was exposed fifty times, Target 2 - 25 times, Target 3 - 25 times, and Target 4 - 25 times. The 125 images were exposed over three different days (a total of four runs) with processing and image evaluation being performed after each day's exposure series. Shutter speeds for the exposures ranged between 1/2 and 1/100 of a second. When 1/100 second provided too high a density in the image, a neutral density filter (0.6 or 1.0) was placed between the light source and the target. These range of exposure times and light intensities were chosen to minimize

reciprocity failure. A complete focus series of exposures was completed before each day's operation to assure consistent calibration of the microcamera.

Image Processing

Image development was carried out in DK-50 developer for eight minutes at 68°F. Standard RIT tray rocking agitation was used. Stop bath was SB-1A for 30 seconds and fix was in F-5 formulation for ten minutes. After a 30-minute wash, the images were bathed in Photo Flo and dried. The entire amount of DK-50 was made in one batch and used on these images four times over a sixteen-day period. Fresh chemicals were used on each of the four runs. Sensitometric step wedges were included on each run and the data is shown in Figure 7.

The processing curve for Run 1 varies most from the curves shown for the other development runs. In choosing the final sixteen images for evaluation, the images from Run 1 were used only as a last resort, when images of the proper density from the other three runs could not be used. Since density was the final criteria for image selection, the variation in the processing should have a minimal effect upon the experimental error. An examination of the data reveals no day-to-day trend.

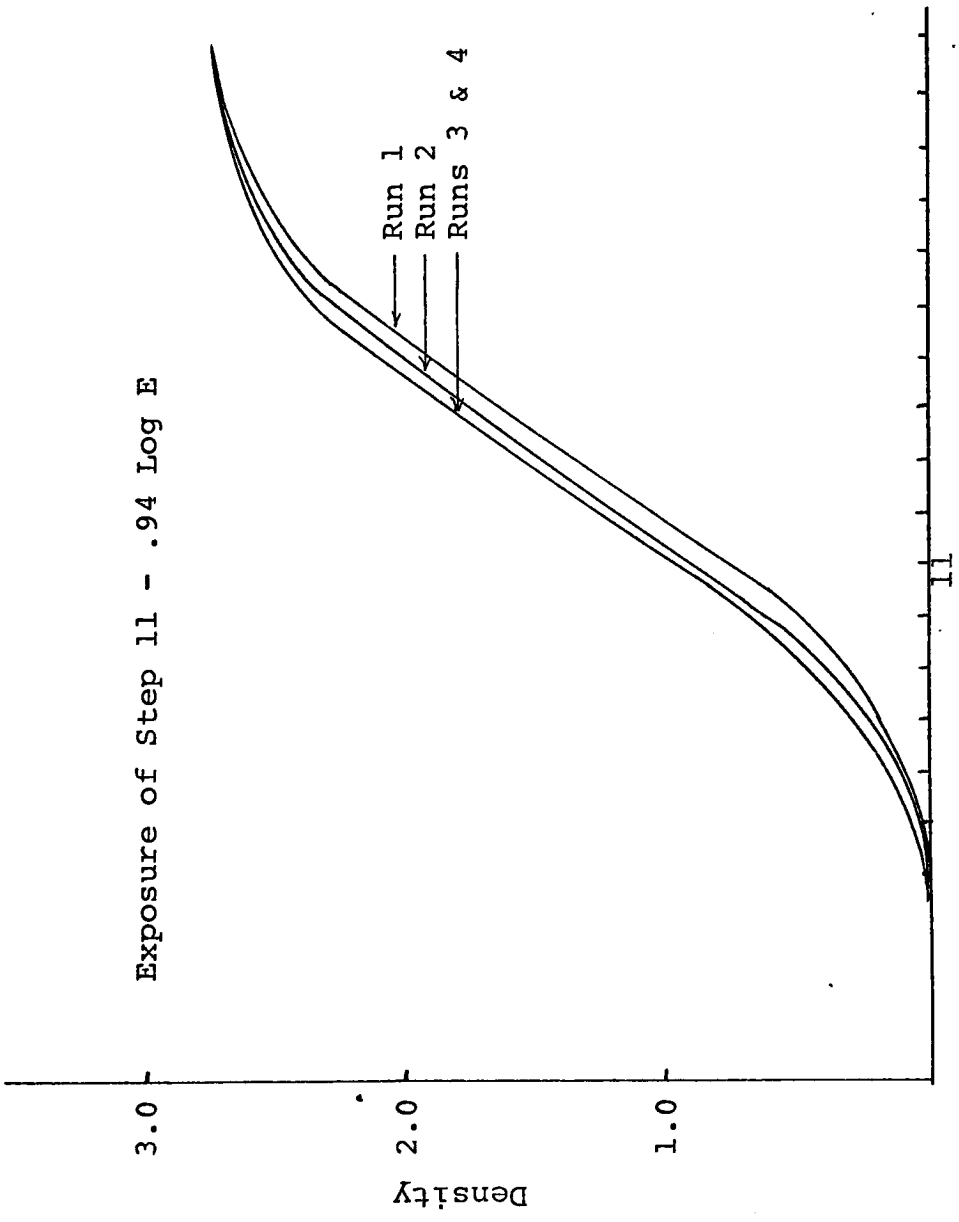

FIGURE 7. Processing Curves for the Images

Image Evaluation

Image densities were determined by the use of a microdensitometer. A Mann microdensitometer, Model 1032 was used. The effective slit aperture was one micrometer wide and 80 micrometers long. The instrument was calibrated for each operating series by reading a 610 cycles/millimeter three-bar resolution target manufactured by Meade Technology Labs. When the instrument could satisfactorily read and record the 610 cycles/millimeter target, the instrument was considered in proper calibration. Densitometric calibration was accomplished using neutral density glass filters before each operating series.

All 125 images were evaluated on the microdensitometer. The procedure was to align each image parallel to the aperture of the microdensitometer, focus and adjust the instrument, and then trace the entire width of the bar. From these 125 traces, the sixteen images (four from each width) of the proper density were chosen. These sixteen images were retraced a second time using extreme care and precision. A trace speed of .125 millimeters per minute was used, and a chart speed of 0.5 inches per second was used. Table 1 shows the pertinent data for each of the sixteen images chosen for the mensuration process.

The sixteen images were then mounted sequentially and in parallel on a 2"x3" clear acetate chip. The order of

the images was random. Double stick Scotch tape was used to secure the base of the images to the acetate. An American Optical Company Dual Stage/Split Field Microscope was used to view the images during mounting. Care was taken to assure the images were parallel, as this would simplify the mensuration procedure for the photogrammetrists. The order of the images is shown in Table 1.

TABLE 1. Order of Position of Images on Acetate Chip

Position in Row	Approximate Target Width (micrometers)	Density	Processing Run which Generated Image
1	100	1.90	3
2	300	1.41	3
3	300	1.90	3
4	50	1.41	2
5	10	1.13	4
6	100	1.08	2
7	10	.40	3
8	50	1.90	1
9	100	.40	1
10	10	1.40	3
11	10	1.91	3
12	300	.45	3
13	300	1.00	1
14	100	1.49	1
15	50	1.10	3
16	50	.44	3

The sixteen images on the chip were then measured visually by five experienced photogrammetrists. Each photogrammetrist repeated every measurement twice. The measurements were made on a David Mann model 1210 comparator. This instrument allows 10 to 160 power magnification, variable illumination, and movable platen.

Platen movement is controlled over the entire field to ±1 micrometer or .001% of travel, whichever is greater, in both an X and Y direction. The operators were allowed to change illumination if desired, but none did and the dial remained in the medium position. Magnification was allowed to be changed but again the operators chose to use only one magnification--120X. This allowed for comfortable viewing and easiest "crosshair" pointing of an edge. The images were presented to the operator in random order. Table 2 gives the order of presentation of the image for each operator measurement series and operator.

TABLE 2. Order of Presentation of Images for Measurement by Photogrammetrists

Measurement Series	Operator	Image 1	2	3	4	5	6	7	8	9	10	11	12	13	14	15	16
1	1	11	3	15	4	5	6	8	1	14	12	2	10	9	16	7	13
1	2	7	13	1	3	11	14	12	16	6	9	8	2	5	4	15	10
1	3	10	5	12	2	11	6	14	16	9	1	7	8	13	4	15	3
1	4	12	1	7	5	13	10	8	11	15	9	14	16	2	4	6	3
1	5	6	4	10	1	8	3	9	16	14	11	15	2	5	12	15	7
2	1	16	2	3	8	15	9	12	5	6	7	13	4	10	11	14	1
2	2	2	9	6	16	5	3	4	15	13	10	8	7	14	16	11	1
2	3	3	5	7	10	6	16	2	4	15	12	15	1	11	8	14	9
2	4	8	16	5	2	3	9	14	11	4	7	1	15	13	6	10	12
2	5	4	14	12	15	9	5	7	1	8	6	16	2	3	10	11	13

The images were placed on the platen of the comparator and aligned parallel to the Y axis. Thus, only the X coordinate needed to be used for the measurement (see Figure 8). Each image was measured by pointing a crosshair to the left edge of the image near the area of the triangle and then to

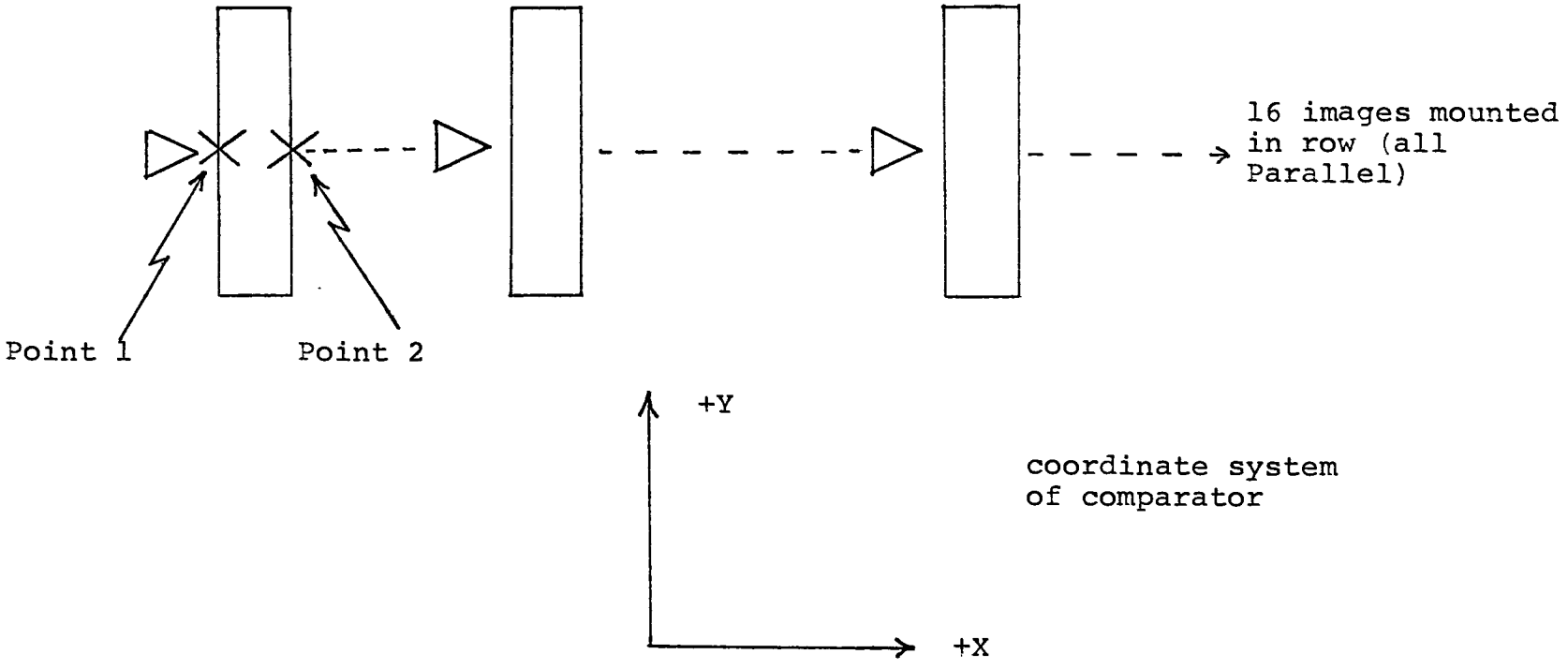

FIGURE 8. Measuring Coordinate System of Comparator Relative to Sixteen Images

the right edge. This procedure was immediately repeated. The two X image coordinates for the left edge were averaged and then the right edge. This was considered as multiple pointing twice. Tables 3, 4, 5, and 6 list the actual comparator image coordinate value for each pointing for each operator. Both measurement series are listed, as well as the multiple pointings (twice) of each edge. The X coordinate of the left edge (average of two pointings) was subtracted from the X coordinate of the right edge to determine the measured width of the image.

Determination of Aerial Image Width

The raw comparator measurements of image width were reduced to the response variable, measurement error so that Analysis of Variance could be performed. Measurement error is defined as the measured image width (data from Table 3-6) minus the actual image width, in this case, the width of the aerial image.

The width of the aerial image was computed by a simple scaling formula:

$$\text{aerial image width} = \frac{\text{input target width}}{\text{reduction factor of micro-camera}}$$

The input target width was determined by measuring the four input targets on the Mann Model 1210 comparator. The same five instrument operators who measured the images measured the input target width. The target widths as measured by each of the five operators is listed in Table 7.

TABLE 3. Comparator Image Coordinate Values for Images From Target One

			IMAGE 7 DENSITY 1 (.40)			IMAGE 5 DENSITY 2 (1.13)			IMAGE 10 DENSITY 3 (1.40)			IMAGE 11 DENSITY 4 (1.91)		
Operator	Measurement Series	Edge	Point 1	Point 2	Average	Point 1	Point 2	Average	Point 1	Point 2	Average	Point 1	Point 2	Average
		1	22181	22182	22181.5	13985	13985	13985.0	31927	31928	31927.5	34926	34926	34926.0
	1	2	22188	22188	22188.0	13992	13992	13992.0	31934	31934	31934.0	34934	34934	34934.0
1		D	7	6	6.5	7	7	7.0	7	6	6.5	8	8	8.0
		1	22184	22184	22184.0	13986	13986	13986.0	31928	31928	31928.0	34928	34928	34928.0
	2	2	22189	22190	22189.5	13992	13992	13992.0	31935	31936	31935.5	34936	34934	34935.0
		D	5	6	5.5	6	6	6.0	7	8	7.5	8	6	7.0
		1	22182	22182	22182.0	13985	13984	13984.5	31927	31928	31927.5	34927	34927	34927.0
	1	2	22190	22191	22190.5	13992	13991	13991.5	31936	31936	31936.0	34935	34934	34934.5
		D	8	9	8.5	7	7	7.0	9	8	8.5	8	7	7.5
2		1	22182	22182	22182.0	13985	13984	13984.5	31928	31929	31928.5	34928	34928	34928.0
	2	2	22190	22190	22190.0	13992	13992	13992.0	31936	31936	31936.0	34935	34935	34935.0
		D	8	8	8.0	7	8	7.5	8	7	7.5	7	7	7.0
		1	22182	22182	22182.0	13986	13987	13986.5	31928	31928	31928.0	34929	34927	34928.0
	1	2	22190	22189	22189.5	13992	13992	13992.0	31936	31936	31936.0	34935	34935	34935.0
		D	8	7	7.5	6	5	5.5	8	8	8.0	6	8	7.0
3		1	22182	22183	22182.5	13986	13986	13986.0	31929	31929	31929.0	34927	34928	34927.5
	2	2	22190	22190	22190.0	13993	13993	13993.0	31936	31936	31936.0	34936	34936	34936.0
		D	8	7	7.5	7	7	7.0	7	7	7.0	9	8	8.5
		1	22181	22182	22181.5	13985	13985	13985.0	31928	31928	31928.0	34928	34928	34928.0
	1	2	22189	22190	22189.5	13992	13993	13992.5	31937	31936	31936.5	34936	34936	34936.0
		D	8	8	8.0	7	8	7.5	9	8	8.5	8	8	8.0
4		1	22182	22182	22182.0	13985	13985	13985.0	31928	31928	31928.0	34928	34928	34928.0
	2	2	22190	22190	22190.0	13994	13994	13994.0	31936	31936	31936.0	34935	34936	34935.5
		D	8	8	8.0	9	9	9.0	8	8	8.0	7	8	7.5
		1	22181	22181	22181.0	13984	13984	13984.0	31927	31927	31927.0	34926	34927	34926.5
	1	2	22188	22189	22188.5	13991	13991	13991.0	31934	31934	31934.0	34934	34935	34934.5
		D	7	8	7.5	7	7	7.0	7	7	7.0	8	8	8.0
5		1	22181	22183	22182.0	13986	13985	13985.5	31928	31928	31928.0	34928	34927	34927.5
	2	2	22189	22190	22189.5	13992	13992	13992.0	31935	31936	31935.5	34936	34937	34936.5
		D	8	7	7.5	6	7	6.5	7	8	7.5	8	10	9.0

TABLE 4. Comparator Image Coordinate Values For Images From Target Two

			IMAGE 16 DENSITY 1 (.44)			IMAGE 15 DENSITY 2 (1.10)			IMAGE 4 DENSITY 3 (1.41)			IMAGE 8 DENSITY 4 (1.90)		
Operator	Measurement Series	Edge	Point 1	Point 2	Average	Point 1	Point 2	Average	Point 1	Point 2	Average	Point 1	Point 2	Average
		1	49804	49805	49804.5	46926	46927	46926.5	9878	9878	9878.0	25052	25053	25052.5
	1	2	49854	49854	49854.0	46976	46976	46976.0	9929	9929	9929.0	25104	25104	25104.0
1		D	50	49	49.5	50	49	49.5	51	51	51.0	52	51	51.5
		1	49809	49810	49809.5	46932	46932	46932.0	9880	9880	9880.0	25054	25054	25054.0
	2	2	49856	49856	49856.0	46979	46978	46978.5	9930	9928	9929.0	25105	25105	25105.0
		D	47	46	46.5	47	46	46.5	50	48	49.0	51	51	51.0
		1	49806	49807	49806.5	46928	46928	46928.0	9878	9878	9878.0	25052	25052	25052.0
	1	2	49856	49856	49856.0	46978	46977	46977.5	9930	9930	9930.0	25104	25104	25104.0
		D	50	49	49.5	50	49	49.5	52	52	52.0	52	52	52.0
2		1	49807	49807	49807.0	46930	46930	46930.0	9880	9879	9879.5	25054	25054	25054.0
	2	2	49856	49855	49855.5	46978	46979	46978.5	9930	9929	9929.5	25100	25103	25101.5
		D	49	48	48.5	48	49	48.5	50	50	50.0	46	49	47.5
		1	49807	49807	49807.0	46928	46928	46928.0	9878	9879	9878.5	25054	25053	25053.5
	1	2	49856	49856	49856.0	46978	46978	46978.0	9929	9929	9929.0	25104	25105	25104.5
		D	49	49	49.0	50	50	50.0	51	50	50.5	50	52	51.0
3		1	49807	49808	49807.5	46929	46930	46929.5	9880	9880	9880.0	25054	25054	25054.0
	2	2	49856	49856	49856.0	46979	46979	46979.0	9931	9931	9931.0	25105	25105	25105.0
		D	49	48	48.5	50	49	49.5	51	51	51.0	51	51	51.0
		1	49806	49805	49805.5	46929	46929	46929.0	9878	9878	9878.0	25053	25054	25053.5
	1	2	49856	49856	49856.0	46978	46978	46978.0	9930	9930	9930.0	25105	25105	25105.0
		D	50	51	50.5	49	49	49.0	52	52	52.0	52	51	51.5
4		1	49805	49806	49805.5	46928	46929	46928.5	9883	9884	9883.5	25054	25054	25054.0
	2	2	49856	49856	49856.0	46979	46980	46979.5	9935	9934	9934.5	25106	25106	25106.0
		D	51	50	50.5	51	51	51.0	52	50	51.0	52	52	52.0
		1	49806	49805	49805.5	46929	46929	46929.0	9878	9878	9878.0	25052	25052	25052.0
	1	2	49855	49854	49854.5	46978	46978	46978.0	9930	9930	9930.0	25104	25104	25104.0
		D	49	49	49.0	49	49	49.0	52	52	52.0	52	52	52.0
5		1	49806	49806	49806.0	46931	46931	46931.0	9879	9880	9879.5	25053	25053	25053.0
	2	2	49856	49856	49856.0	46980	46980	46980.0	9931	9930	9930.5	25106	25105	25105.5
		D	50	50	50.0	49	49	49.0	52	50	51.0	53	52	52.5

TABLE 5. Comparator Image Coordinate Values For Images From Target Three

			IMAGE 9 DENSITY 1 (.40)			IMAGE 6 DENSITY 2 (1.08)			IMAGE 14 DENSITY 3 (1.49)			IMAGE 1 DENSITY 4 (1.90)		
Operator	Measurement Series	Edge	Point 1	Point 2	Average	Point 1	Point 2	Average	Point 1	Point 2	Average	Point 1	Point 2	Average
		1	28506	28505	28505.5	17918	17918	17918.0	44193	44192	44192.5	167	168	167.5
	1	2	28596	28595	28595.5	18012	18012	18012.0	44288	44288	44288.0	262	261	261.5
1		D	90	90	90.0	94	94	94.0	95	96	95.5	95	93	94.0
		1	28508	28509	28508.5	17921	17920	17920.5	44196	44196	44196.0	166	167	166.5
	2	2	28595	28596	28595.5	18012	18013	18012.5	44290	44290	44290.0	258	259	258.5
		D	87	87	87.0	91	93	92.0	94	94	94.0	92	92	92.0
		1	28505	28504	28504.5	17918	17918	17918.0	44195	44195	44195.0	167	167	167.0
	1	2	28596	28596	28596.0	18014	18012	18013.0	44290	44289	44289.5	262	260	261.0
		D	91	92	91.5	96	94	95.0	95	94	94.5	95	93	94.0
2		1	28506	28505	28505.5	17918	17918	17918.0	44197	44196	44196.5	169	170	169.5
	2	2	28597	28596	28596.5	18013	18012	18012.5	44289	44289	44289.0	257	257	257.0
		D	91	91	91.0	95	94	94.5	92	93	92.5	88	87	87.5
		1	28506	28505	28505.5	17918	17919	17918.5	44195	44194	44194.5	168	168	168.0
	1	2	28595	28598	28596.5	18012	18012	18012.0	44290	44291	44290.5	259	260	259.5
		D	89	93	91.0	94	93	93.5	95	97	96.0	91	92	91.5
3		1	28507	28506	28506.5	17918	17918	17918.0	44194	44195	44194.5	168	167	167.5
	2	2	28595	28595	28595.0	18014	18014	18014.0	44289	44289	44289.0	260	260	260.0
		D	88	89	88.5	96	96	96.0	95	94	94.5	92	93	92.5
		1	28505	28505	28505.0	17918	17918	17918.0	44194	44195	44194.5	166	166	166.0
	1	2	28596	28596	28596.0	18013	18013	18013.0	44290	44289	44289.5	261	261	261.0
		D	91	91	91.0	95	95	95.0	96	94	95.0	95	95	95.0
4		1	28505	28504	28504.5	17919	17919	17919.0	44194	44195	44194.5	166	166	166.0
	2	2	28596	28596	28596.0	18014	18014	18014.0	44289	44290	44289.5	261	260	260.5
		D	91	92	91.5	95	95	95.0	95	95	95.0	95	94	94.5
		1	28504	28503	28503.5	17916	17918	17917.0	44193	44194	44193.5	166	166	166.0
	1	2	28594	28595	28594.5	18013	18013	18013.0	44289	44289	44289.0	259	258	258.5
		D	90	92	91.0	97	95	96.0	96	95	95.5	93	92	92.5
5		1	28507	28506	28506.5	17919	17918	17918.5	44195	44195	44195.0	166	166	166.0
	2	2	28597	28597	28597.0	18014	18014	18014.0	44291	44291	44291.0	261	261	261.0
		D	90	91	90.5	95	96	95.5	96	96	96.0	95	95	95.0

TABLE 6. Comparator Image Coordinate Values For Images From Target Four

			IMAGE 12			IMAGE 13			IMAGE 2			IMAGE 3		
			DENSITY 1 (.45)			DENSITY 2 (1.00)			DENSITY 3 (1.41)			DENSITY 4 (1.90)		
Operator	Measurement Series	Edge	Point 1	Point 2	Average	Point 1	Point 2	Average	Point 1	Point 2	Average	Point 1	Point 2	Average
		1	37788	37789	37788.5	41250	41249	41249.5	3233	3233	3233.0	6355	6356	6355.5
	1	2	38078	38080	38079.0	41544	41544	41544.0	3527	3527	3527.0	6648	6650	6649.0
1		D	290	291	290.5	294	295	294.5	294	294	294.0	293	294	293.5
		1	37791	37791	37791.0	41253	41254	41253.5	3234	3234	3234.0	6357	6357	6357.0
	2	2	38079	38081	38080.0	41545	41546	41545.5	3527	3526	3526.5	6650	6649	6649.5
		D	288	290	289.0	292	292	292.0	293	292	292.5	293	292	292.5
		1	37788	37790	37789.0	41253	41252	41252.5	3233	3233	3233.0	6356	6357	6356.5
	1	2	38079	38078	38078.5	41545	41546	41545.5	3528	3527	3527.5	6649	6650	6649.5
		D	291	288	289.5	292	294	293.0	295	294	294.5	293	293	293.0
2		1	37789	37788	37788.5	41255	41255	41255.0	3234	3234	3234.0	6361	6362	6361.5
	2	2	38081	38078	38079.5	41544	41543	41543.5	3527	3527	3527.0	6647	6647	6647.0
		D	292	290	291.0	289	288	288.5	293	293	293.0	286	285	285.5
		1	37789	37791	37790.0	41252	41254	41253.0	3235	3233	3234.0	6356	6356	6356.0
	1	2	38079	38078	38078.5	41543	41545	41544.0	3527	3528	3527.5	6649	6648	6648.5
		D	290	287	288.5	291	291	291.0	292	295	293.5	293	292	292.5
3		1	37788	37788	37788.0	41253	41253	41253.0	3235	3234	3234.5	6359	6358	6358.5
	2	2	38079	38079	38079.0	41543	41545	41544.0	3529	3529	3529.0	6651	6651	6651.0
		D	291	291	291.0	290	292	291.0	294	295	294.5	292	293	292.5
		1	37789	37789	37789.0	41251	41251	41251.0	3233	3233	3233.0	6356	6355	6355.5
	1	2	38080	38079	38079.5	41546	41546	41546.0	3528	3528	3528.0	6648	6649	6648.5
		D	291	290	290.5	295	295	295.0	295	295	295.0	292	294	293.0
4		1	37785	37786	37785.5	41249	41248	41248.5	3234	3234	3234.0	6358	6358	6358.0
	2	2	38080	38080	38080.0	41547	41548	41547.5	3530	3529	3529.5	6650	6650	6650.0
		D	295	294	294.5	298	300	299.0	296	295	295.5	292	292	292.0
		1	37788	37788	37788.0	41250	41252	41251.0	3232	3232	3232.0	6356	6356	6356.0
	1	2	38078	38078	38078.0	41544	41543	41543.5	3528	3528	3528.0	6648	6648	6648.0
		D	290	290	290.0	294	291	292.5	296	296	296.0	292	292	292.0
5		1	37790	37789	37789.5	41251	41251	41251.0	3234	3234	3234.0	6358	6357	6357.5
	2	2	38078	38080	38079.0	41544	41542	41543.5	3530	3529	3539.5	6651	6652	6651.5
		D	288	291	289.5	293	292	292.5	296	295	295.5	293	295	294.0

TABLE 7. Input Target Width in Micrometers Measured by Five Operators

Operator	Target 1	2	3	4
1	541	3782	7360	22918
2	541	3785	7364	22943
3	536	3783	7349	22946
4	533	3783	7332	22922
5	536	3782	7360	22926
$\bar{x}$	537.4	3783.0	7353.0	22931.0

Data did not exist as to the precise reduction factor of the microcamera. The following experimental technique and formula were utilized to determine the microcamera reduction factor.

$$\text{Reduction Factor} = \frac{\text{Length of Input Target}}{\text{Length of image of target on film}}$$

Long dimensions (length of input target and image) were utilized so that edge pointing errors are not a significant factor in determining the reduction factor. Since comparable point selection was important here, rather than an interpretation by several operators of where the edge was, only one operator was used. Comparable points between the object and image were determined by the operator who made the measurements, and a second operator who visually verified them. Table 8 lists the length of the input target, right and left side, lengths of the resulting image, right and left side, and finally, the reduction factor computed from each measurement.

TABLE 8. Length of Input Target and Corresponding Image (in micrometers) and Reduction Factor of Microcamera

	INPUT TARGET	IMAGE	REDUCTION FACTOR
Target 1 - right side	54151.00	698.10	77.57
Target 1 - left side	54161.01	698.10	77.58
Target 2 - right side	43581.08	568.00	76.73
Target 2 - left side	43589.01	571.01	76.34
Target 3 - right side	43850.28	559.02	78.44
Target 3 - left side	43909.01	561.01	78.27
Target 4 - right side	57230.02	729.00	78.50
Target 4 - left side	59989.01	733.00	77.75

The variability of the reduction factor determined from each target was considered as part of the experimental error and the one number used as the reduction factor was the average of these eight individual determinations, 77.647. By dividing the average measured target width in Table 7 by the reduction factor, the aerial image width, in micrometers is determined; i.e., Target 1, 6.9; Target 2, 48.7; Target 3, 94.7; and Target 4, 295.3.

TABLE 9. Measurement Error in Micrometers

Image Width	6.9				48.7				94.7				295.3					
Image Density	.40	1.13	1.40	1.91	.44	1.10	1.41	1.90	.40	1.08	1.49	1.90	.45	1.00	1.41	1.90	SUM	MEAN
Operator	-0.4	+0.1	-0.4	+1.1	+0.8	+0.8	+2.3	+2.8	-4.7	-0.7	+0.8	-0.7	-4.8	-0.8	-1.3	-1.8	-38.9	-1.22
1	-1.4	-0.9	+0.6	-0.9	-2.2	-2.2	+1.7	+2.3	-7.7	-2.7	-0.7	-2.7	-6.3	-3.3	-2.8	-2.8		
2	+1.6	+0.1	+1.6	+0.6	+0.8	+0.8	+3.3	+3.3	-3.2	+0.3	-0.2	-0.7	-5.8	-2.3	-0.8	-2.3	-37.3	-1.17
	+1.1	+0.6	+0.6	+0.1	-0.2	-0.2	+1.3	-1.2	-3.7	-0.2	-2.2	-7.2	-4.3	-6.8	-2.3	-9.8		
3	+0.6	-1.4	+1.1	+0.1	+0.3	+1.3	+1.8	+2.3	-3.7	-1.2	+1.3	-3.2	-6.8	-4.3	-1.8	-2.8	-26.3	-0.82
	+0.6	+0.1	+0.1	+1.6	-0.2	+0.8	+2.3	+2.3	-6.2	+1.3	-0.2	-2.2	-4.3	-4.3	-0.8	-2.8		
4	+1.1	+0.6	+1.6	+1.1	+1.8	+0.3	+3.3	+2.8	-3.7	+0.3	+0.3	+0.3	-4.8	-0.3	-0.3	-2.3	+13.2	+.41
	+1.1	+2.1	+1.1	+0.6	+1.8	+2.3	+2.3	+3.3	-3.2	+0.3	+0.3	-0.2	-0.8	+3.7	-0.3	-3.3		
5	+0.6	+0.1	+0.1	+1.1	+0.3	+0.3	+3.3	+3.3	-3.7	+1.3	+0.8	-2.2	-5.3	-2.8	+0.7	-3.3	-6.3	-.20
	+0.6	-0.4	+0.6	+2.1	+1.3	+0.3	+2.3	+3.8	-4.2	+0.8	+1.3	+0.3	-5.8	-2.8	+0.2	-1.3		
Sum	+5.5	+1.0	+7.0	+7.5	+4.5	+4.5	+23.9	+25.0	-44.0	-0.5	+1.5	-18.5	-49.0	-24.0	-9.5	-32.5		
Mean	+.55	+.10	+.70	+.75	+.45	+.45	+2.39	+2.50	-4.40	-.05	+.15	-1.85	-4.90	-2.40	-.95	-3.25		

Table Value = Measured - Actual

Statistical Analysis

This project was designed as a three factor, fully crossed, and twice replicated experiment to be analyzed by Analysis of Variance techniques. The final assemblage of data is given in Table 9. The response variable - measurement error, was determined by subtracting the aerial image width of each target from the measured width on film of each target.

A detailed statistical analysis is shown in the appendix. The ANOVA table resulting from that statistical analysis is shown in Table 10.

TABLE 10. Analysis of Variance

Source	Sum of Squares	Variance	Mean Square	F Ratio	F (.01) Table
Operator (O)	62.95	4	15.74	9.26*	3.49-S
Width (W)	460.49	3	153.50	12.09	6.99-S
Density (D)	143.39	3	47.80	3.76	6.99-NS
O X W	22.97	12	1.91	1.12*	2.35-NS
O X D	36.86	12	3.07	1.81*	2.35-NS
D X W	114.33	9	12.70	7.47*	2.57-S
O X W X D	47.59	36	1.32	0.71	1.94-NS
Error	149.18	80	1.86		
Total	1037.76	159			

*F ratio determined from pooled error of OXWXD and experimental error term.

RESULTS

Statistical Analysis

The rigorous statistical analysis has indicated the following results:

1. There is a significant difference in measurement error when different operators are used in the measurement process.

2. There is a significant difference in measurement error when different image widths are used in the experiment.

3. There is no significant difference in measurement error when different image densities are used in the experiment. (This will be discussed in detail later, since it does not agree with the theory of the imaging process.)

4. There is no significant interaction between operators and image width.

5. There is no significant interaction between operators and image density.

6. There is a significant interaction between image width and image density.

7. There is no significant interaction among operator, image width, and image density.

Graphical Analysis

The microdensitometer traces of each of the sixteen images are shown in Figures 9-24. One small block in the X direction represents 0.05 density unit. The box indicators (⊔⊔) along the bottom of the graphs represent the endpoints, and plus or minus one standard deviation, of the computed width of the aerial image. The (+) sign on the microdensitometer trace indicates the endpoints of the average width computed from ten measurements (five operators X two replicates). The plotting of the measured width on the microdensitometer trace assumes a symmetric placement of the endpoints with respect to the trace, i.e., the operator selected the same density level for pointing at each end of the measurement. A visual examination of the raw data indicates this to be generally the case but there are exceptions. This experiment was not designed to detect nonsymmetric edge pointing when comparing the left edge to the right edge. The (⊕) on the microdensitometer trace indicates the range of the endpoint selection for the ten measurements. In order to easily display the twelve traces from the three widest images, (Figures 12-24) only the edges are shown in the graph. The central section of the trace has been extracted and the edges brought closer together. The number in micrometers in the central, clear portion of the graphs

indicates the width on the film which was represented by the extracted portion of the original microdensitometer trace.

A summary of measurement data is given in Table 11.

TABLE 11. Summary of Measurement Data for Sixteen Images

Aerial Image Width	Image Density	Average of Ten Measurements	Range of Ten Measurements
6.9	.40	7.4	5.5 - 8.5
6.9	1.13	7.0	5.5 - 9.0
6.9	1.40	7.6	6.5 - 8.5
6.9	1.91	7.7	6.0 - 9.0
48.7	.44	49.2	46.5 - 50.5
48.7	1.10	49.2	46.5 - 51.0
48.7	1.41	51.1	49.0 - 52.0
48.7	1.90	51.3	47.5 - 52.5
94.7	.40	90.3	87.0 - 91.5
94.7	1.08	94.9	92.0 - 96.0
94.7	1.49	94.7	92.5 - 96.0
94.7	1.90	91.7	87.5 - 95.0
295.3	.45	290.4	288.5 - 294.5
295.3	1.00	292.9	288.5 - 299.0
295.3	1.41	294.3	292.5 - 296.0
295.3	1.90	292.1	285.5 - 294.0

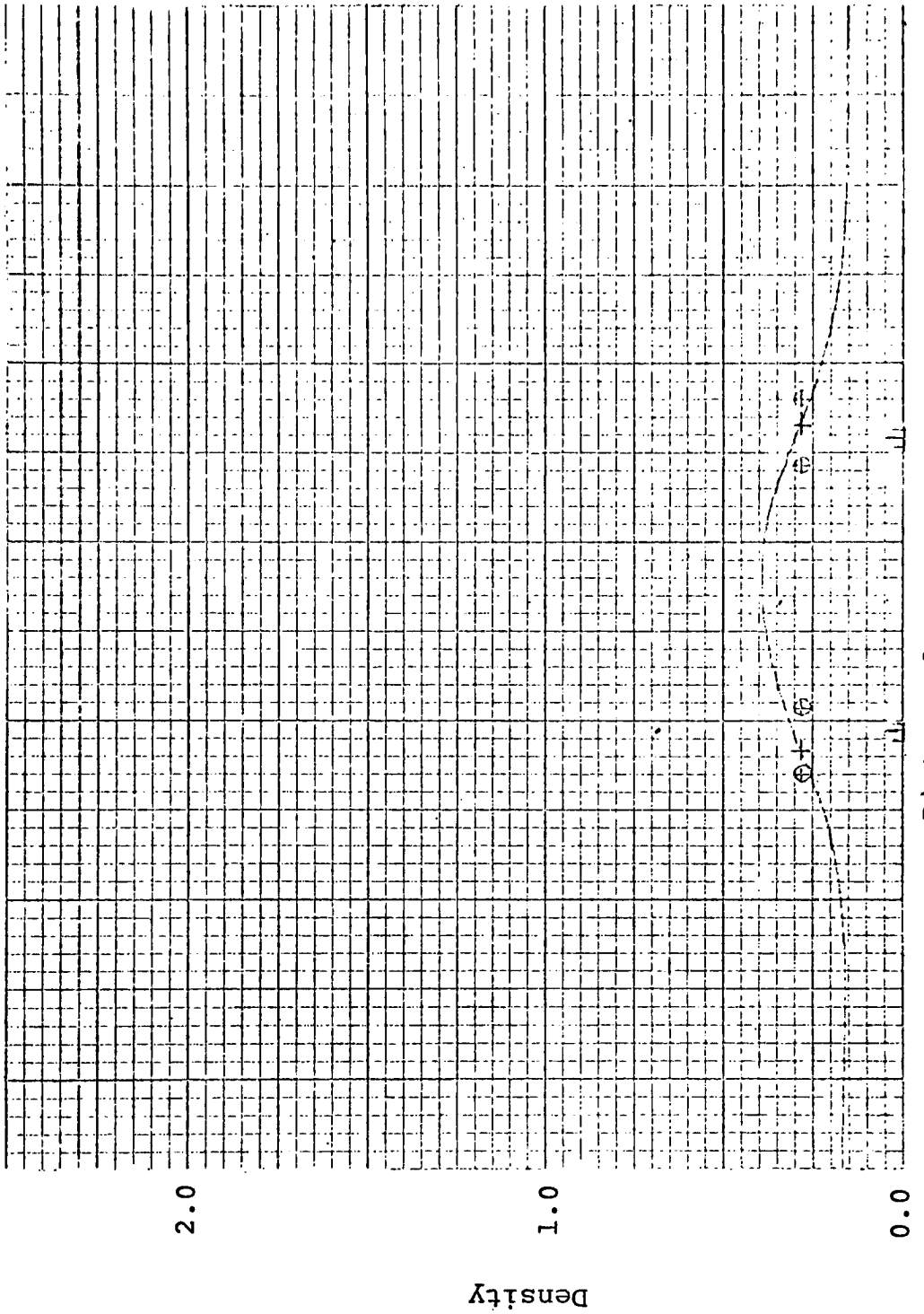

FIGURE 9. Microdensitometer Trace of 6.9 Micrometer Wide Image, 0.39 Density Maximum.

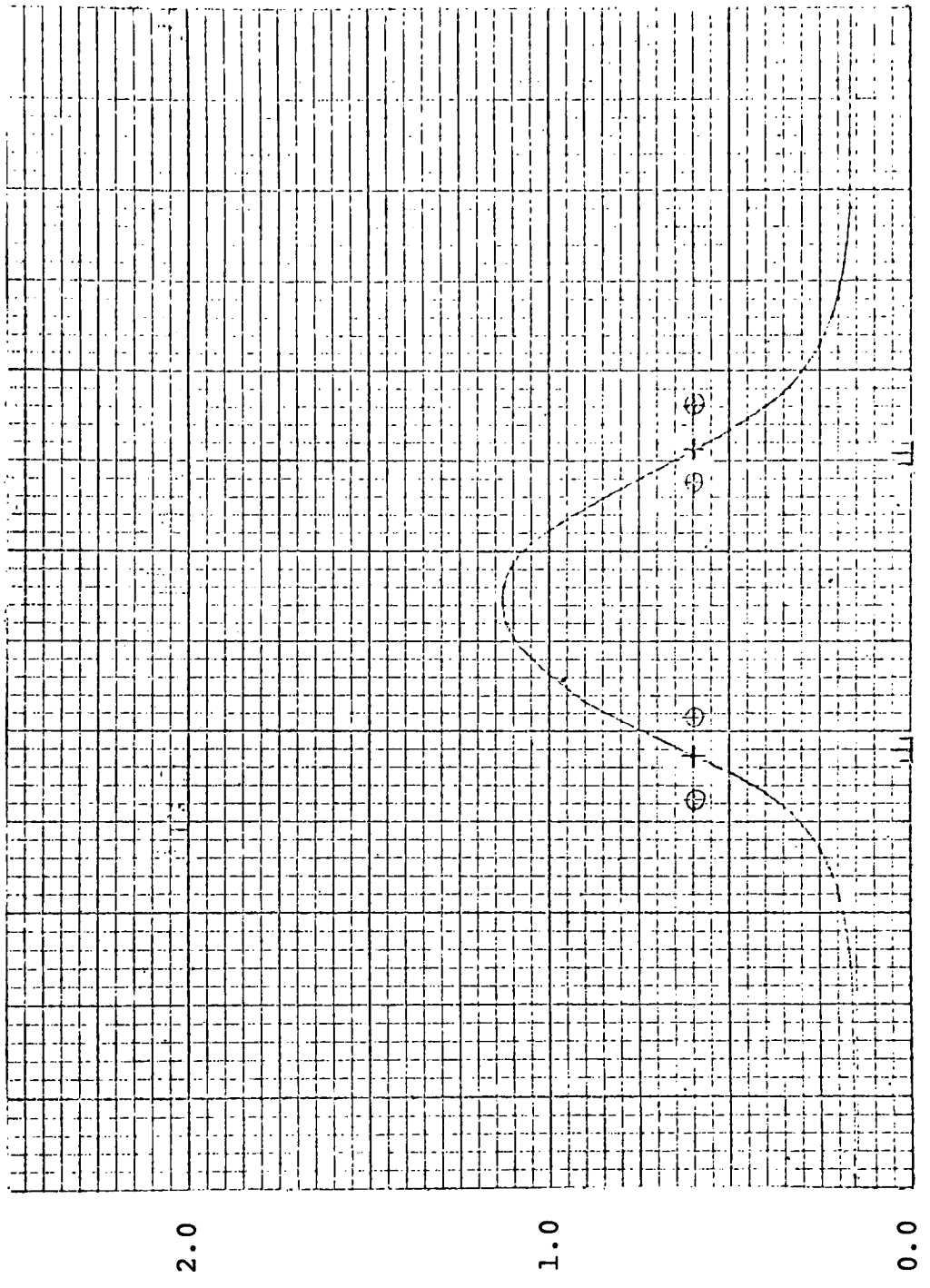

FIGURE 10. Microdensitometer Trace of 6.9 Micrometer Wide Image, 1.13 Density Maximum

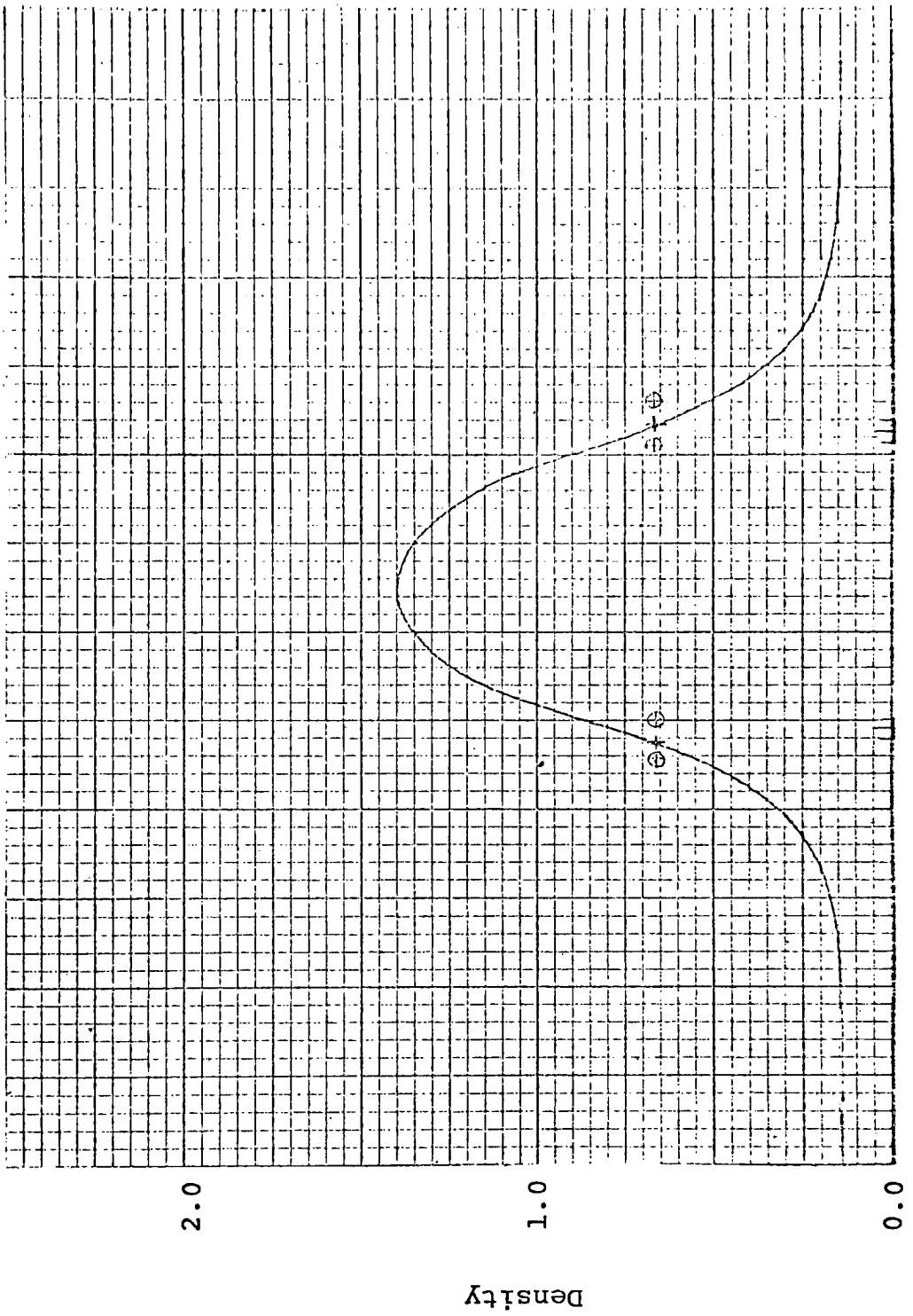

FIGURE 11. Microdensitometer Trace of 6.9 Micrometer Wide Image, 1.40 Density Maximum

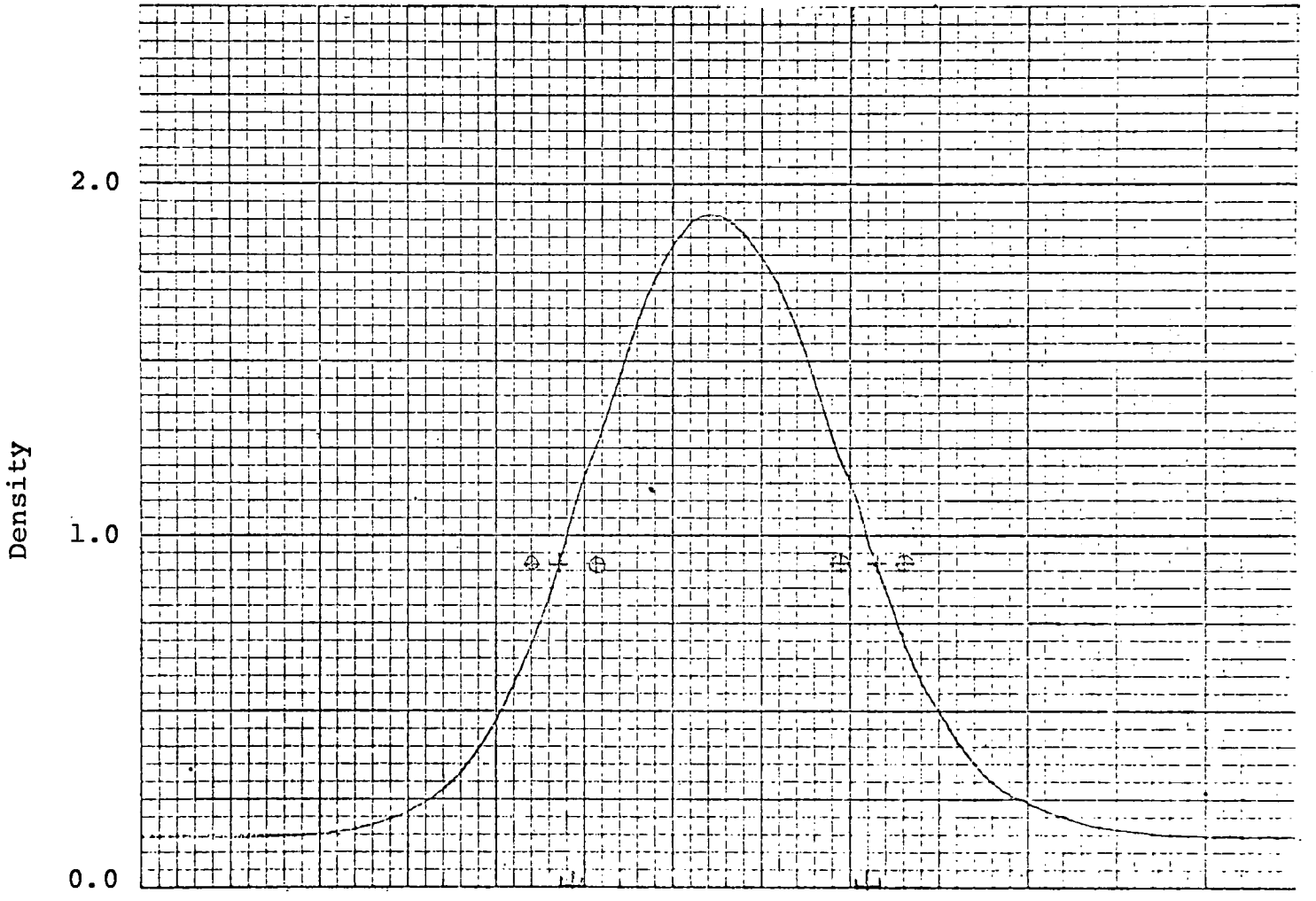

FIGURE 12. Microdensitometer Trace of 6.9 Micrometer Wide Image, 1.91 Density Maximum

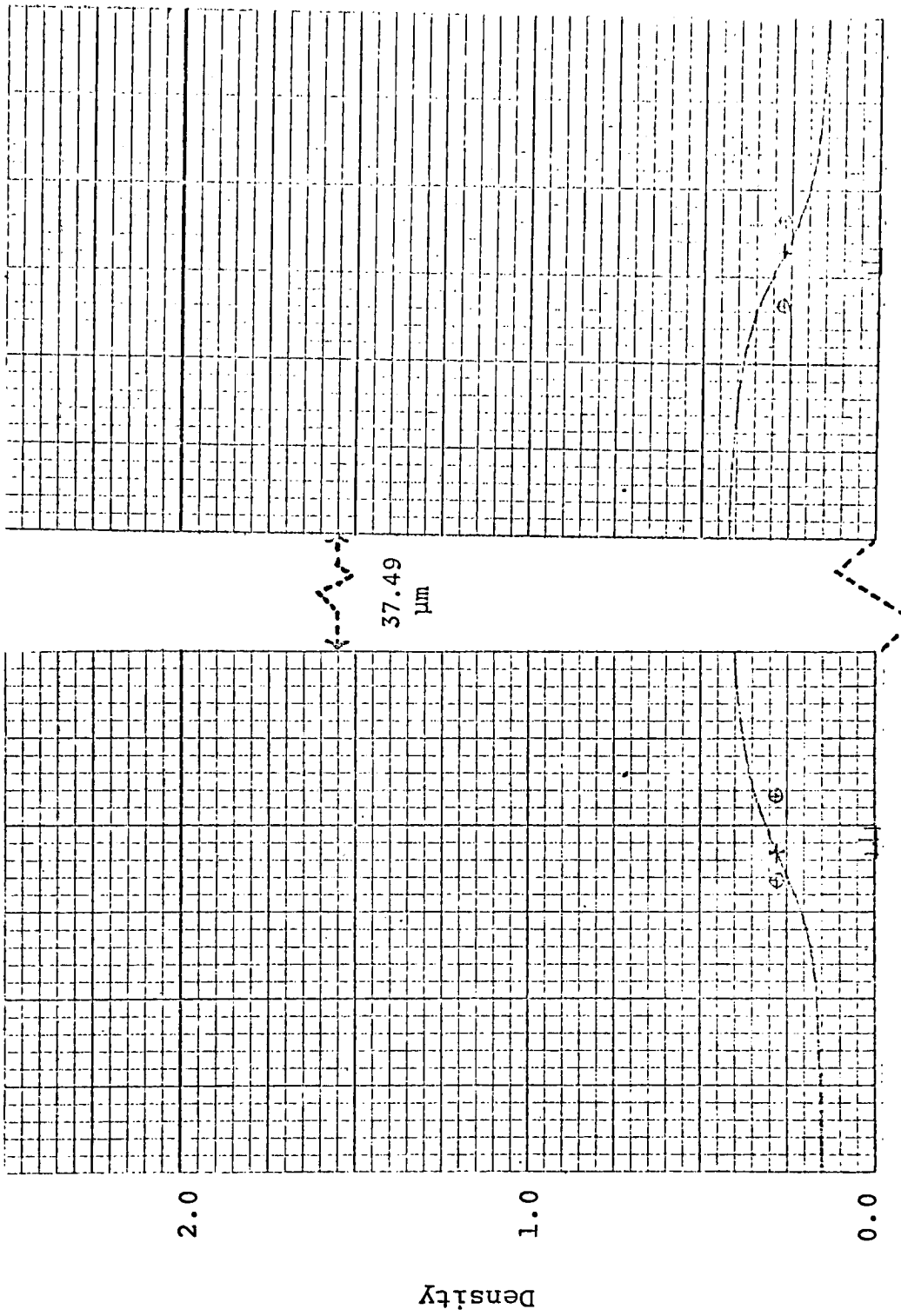

FIGURE 13. Microdensitometer Trace of 48.7 Micrometer Wide Image, 0.41 Density Maximum

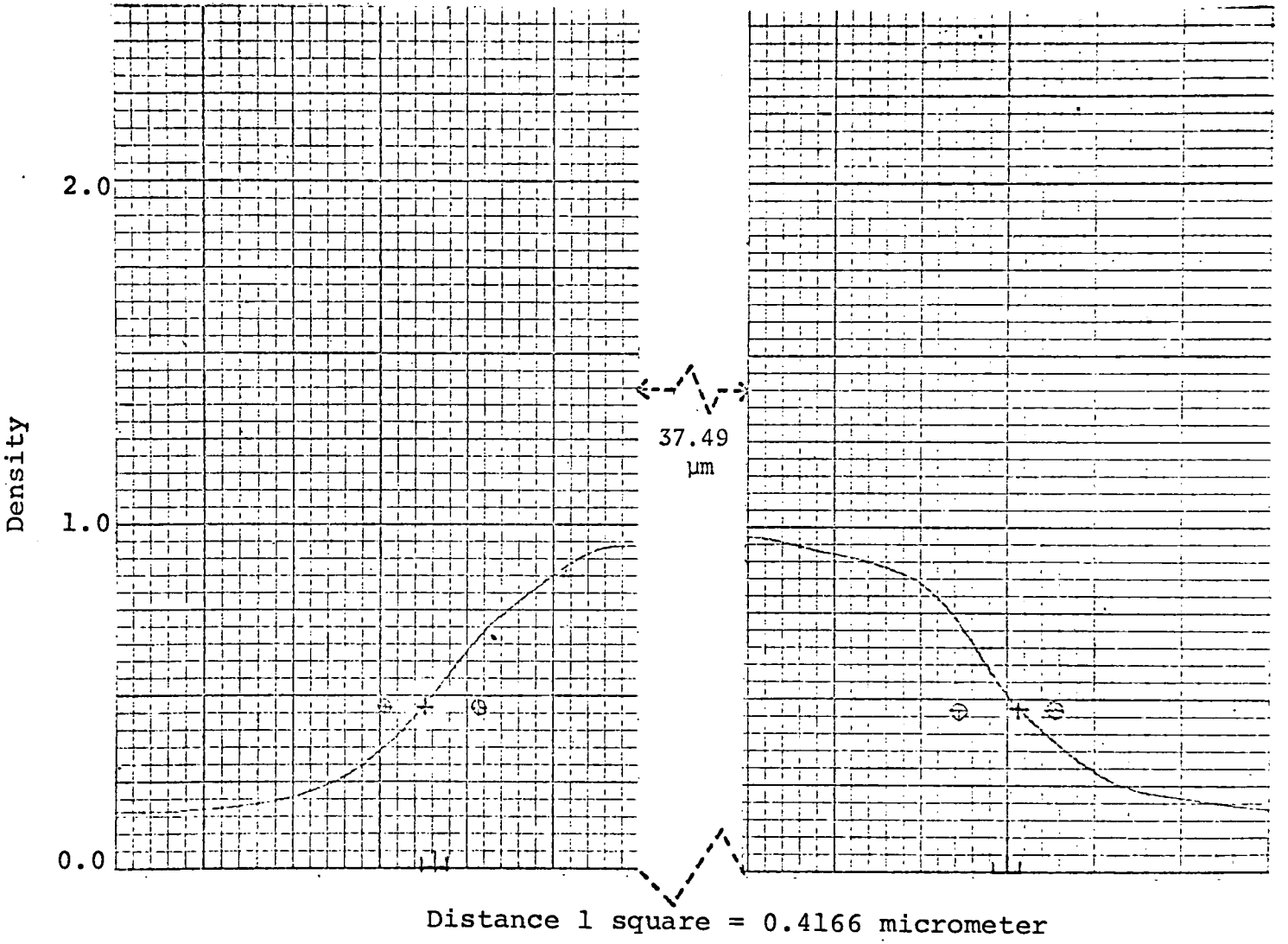

FIGURE 14. Microdensitometer Trace of 48.7 Micrometer Wide Image, 1.00 Density Maximum

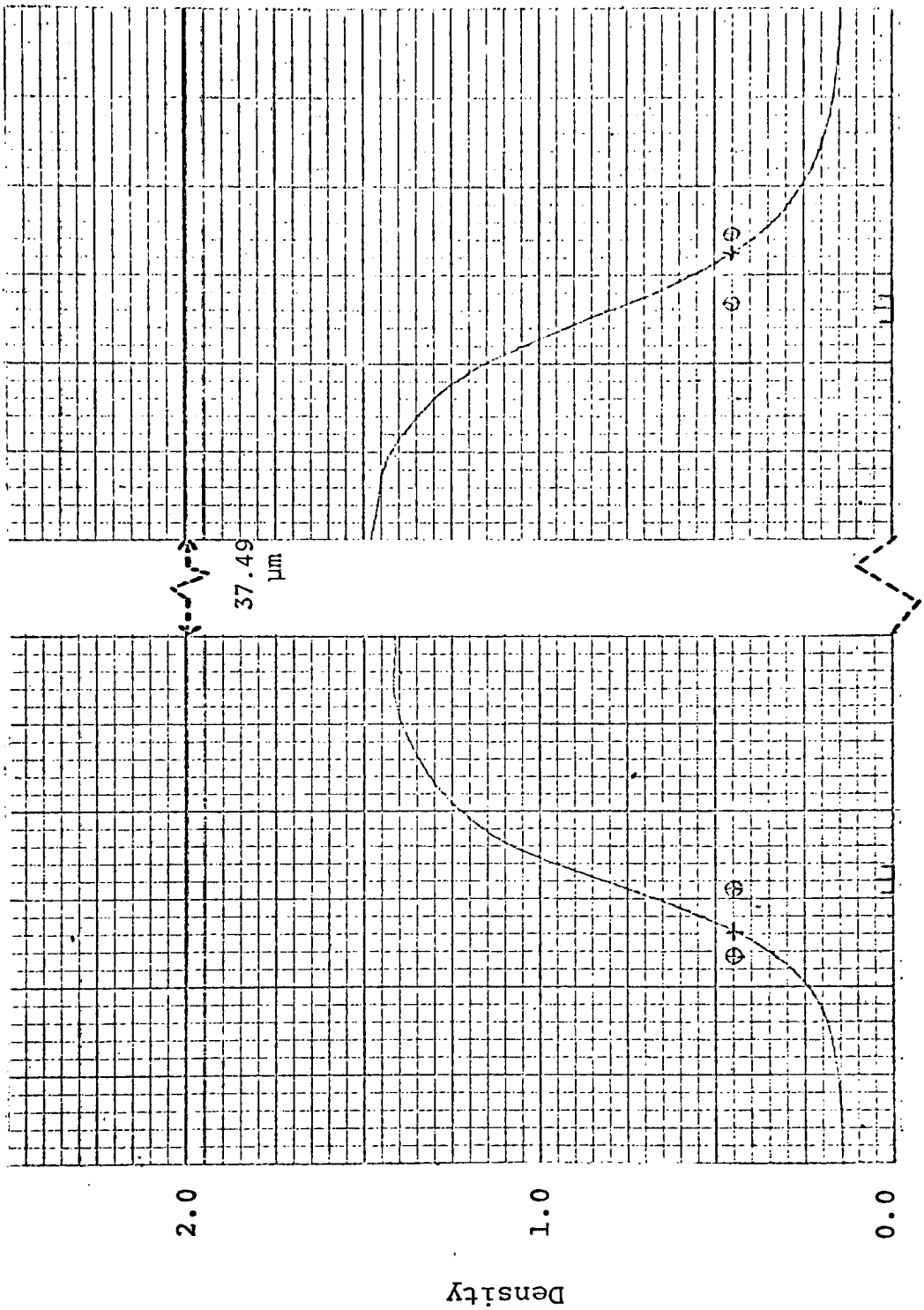

FIGURE 15. Microdensitometer Trace of 48.7 Micrometer
Wide Image, 1.41 Density Maximum

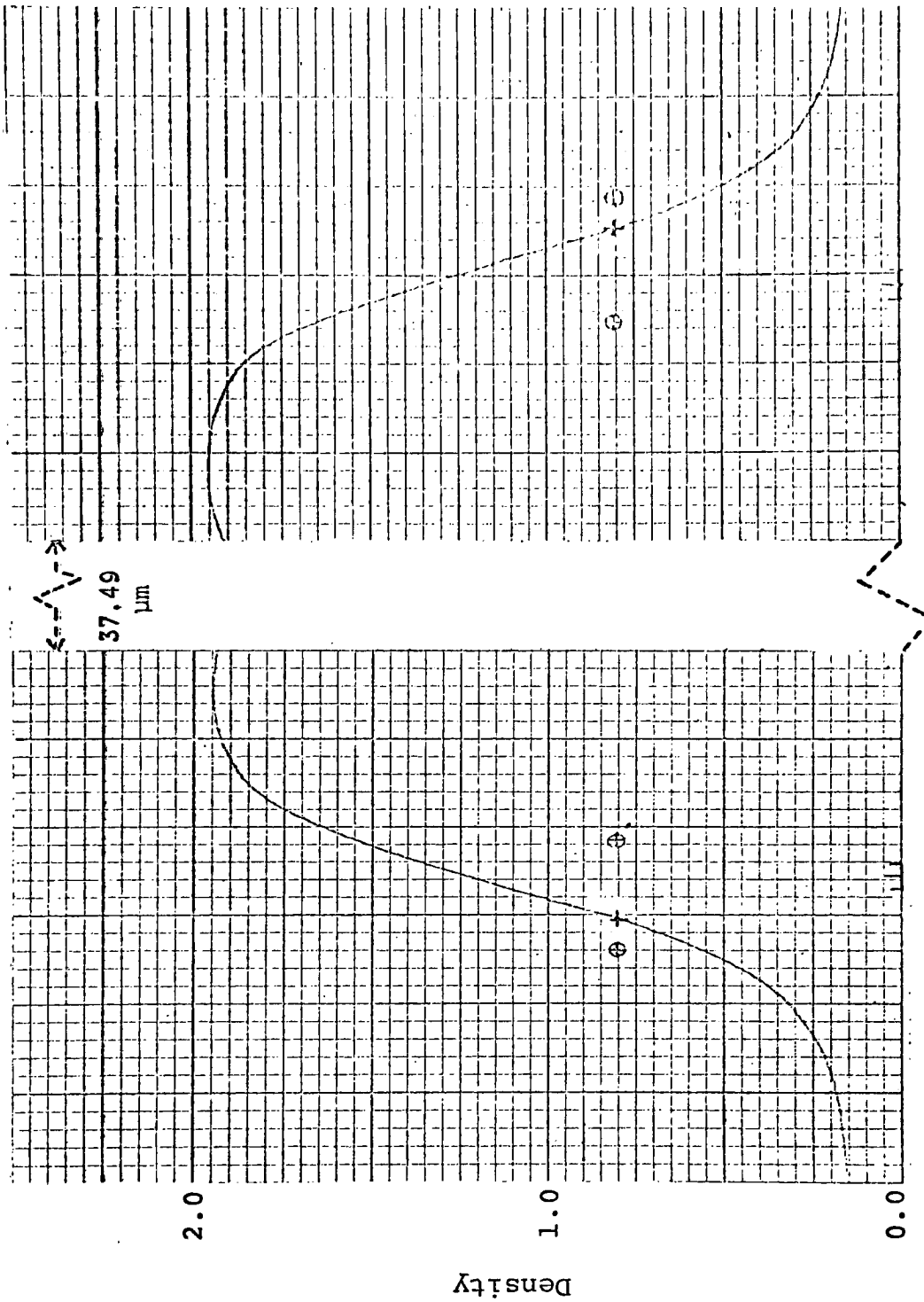

Distance 1 square = 0.4166 micrometer

FIGURE 16. Microdensitometer Trace of 48.7 Micrometer Wide Image, 1.90 Density Maximum

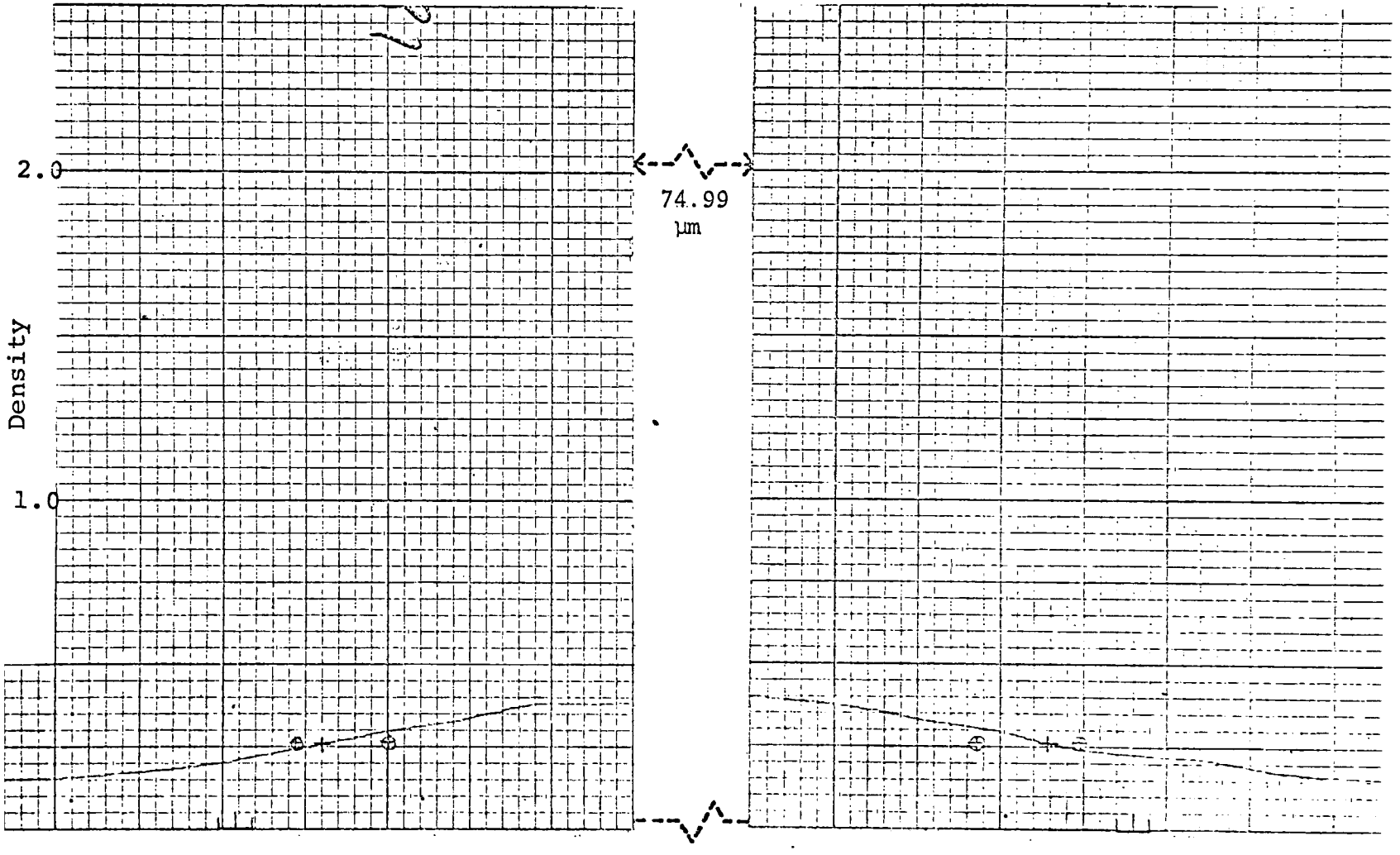

Distance 1 square = 0.4166 micrometer

GURE 17. Microdensitometer Trace of 94.7 Micrometer Wide Image, 0.40 Density Maximum

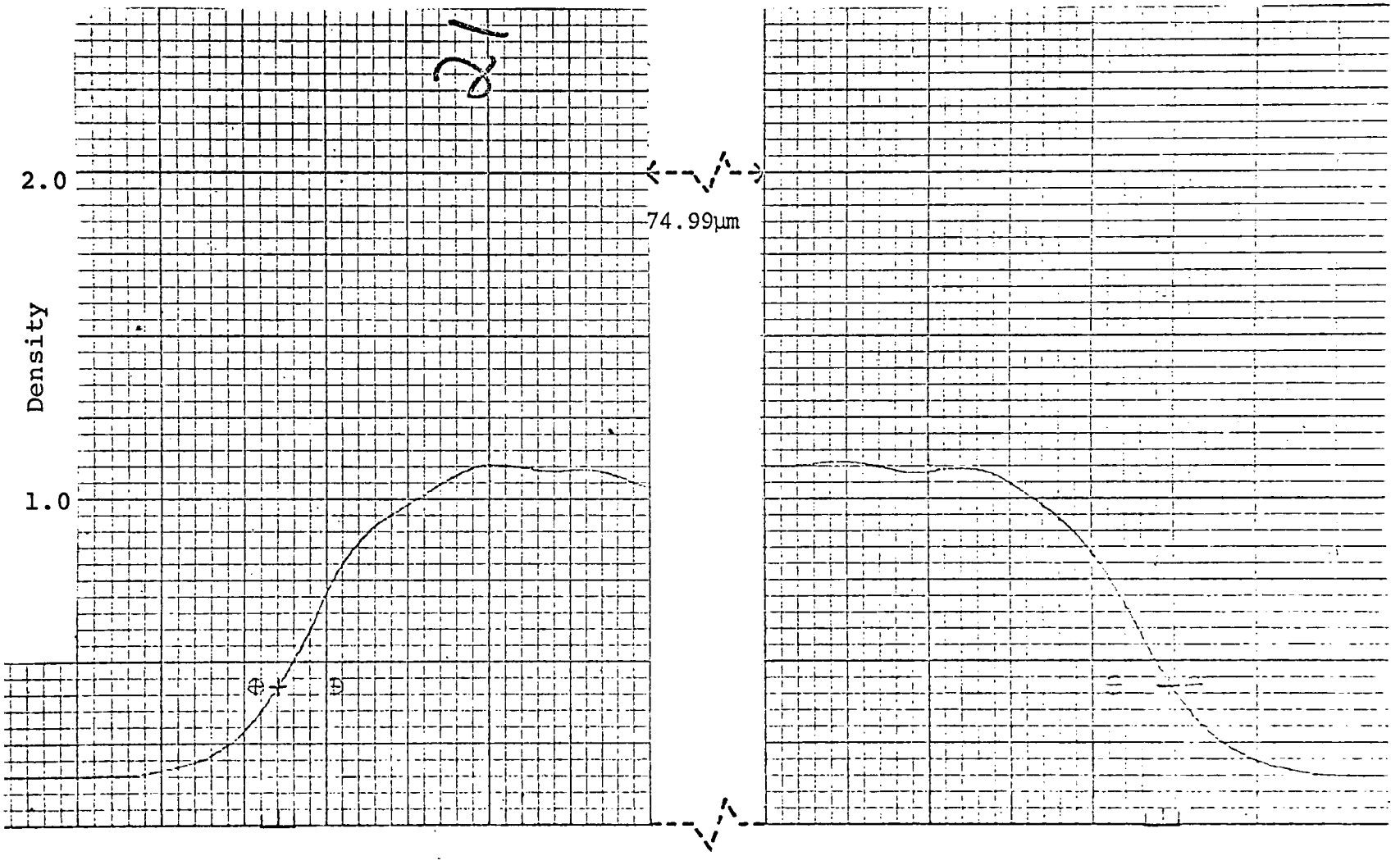

FIGURE 18. Microdensitometer Trace of 94.7 Micrometer Wide Image, 1.08 Density Maximum

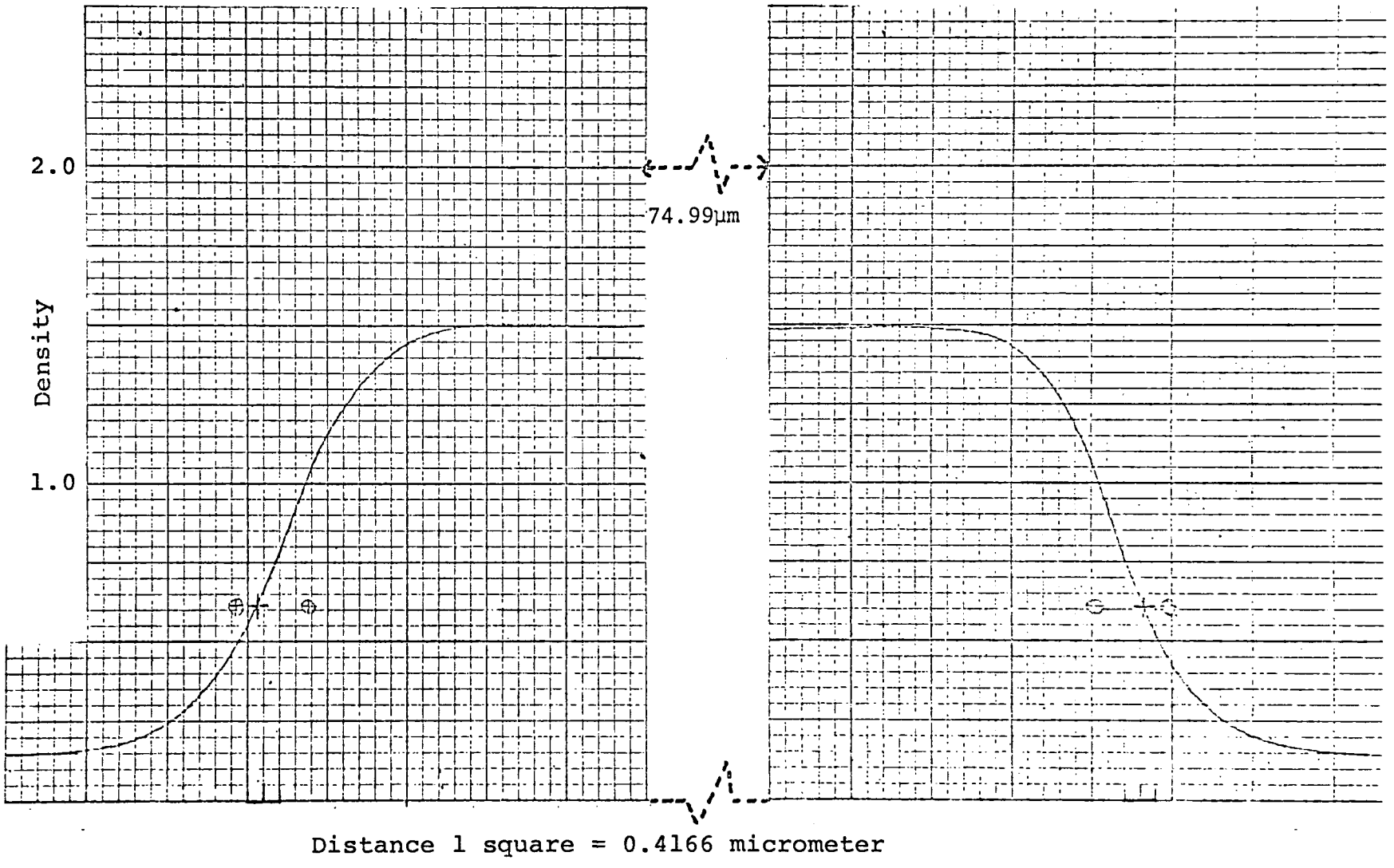

FIGURE 19. Microdensitometer Trace of 94.7 Micrometer Wide Image, 1.49 Density Maximum

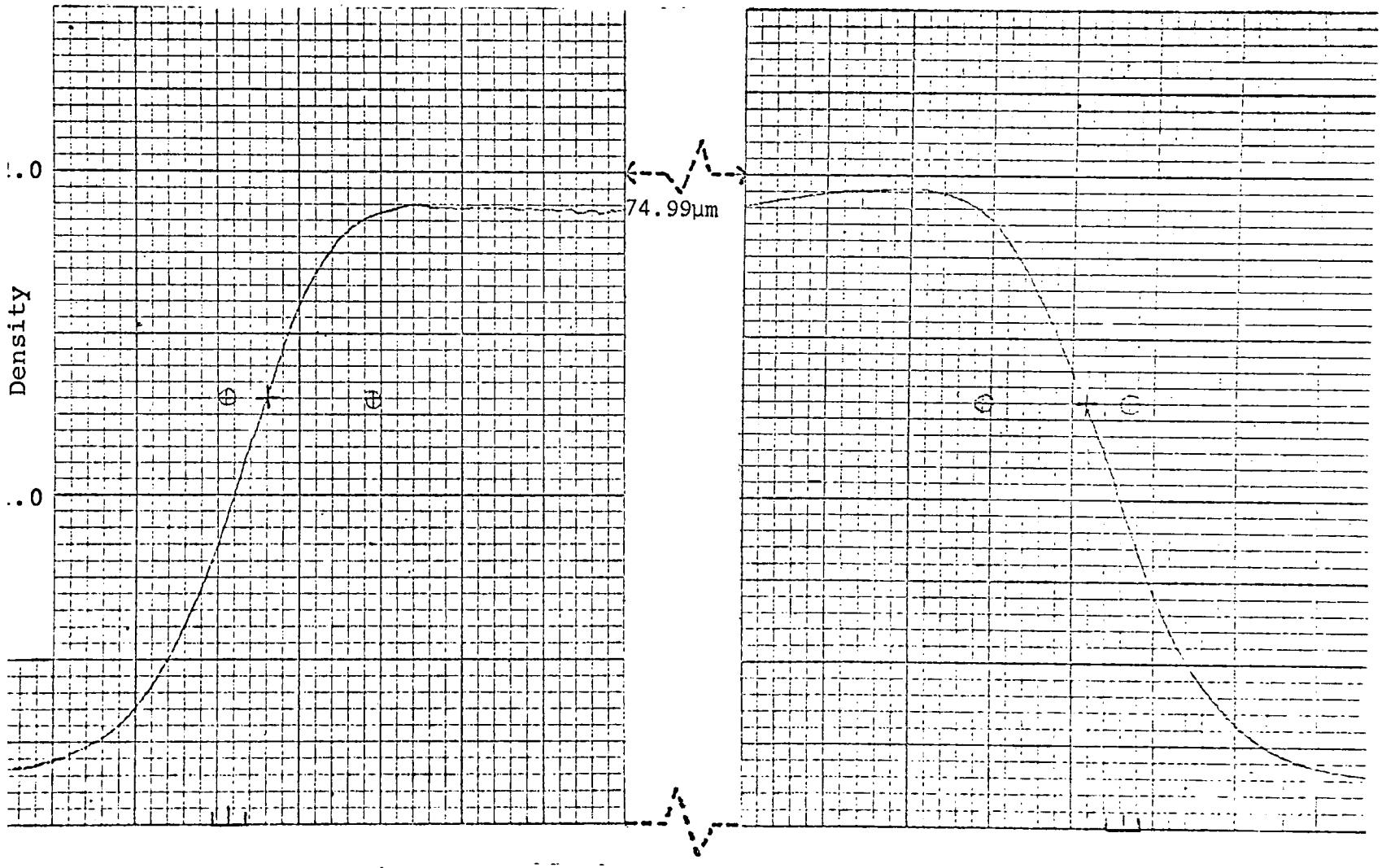

GURE 20. Microdensitometer Trace of 94.7 Micrometer Wide Image, 1.90 Density Maximum

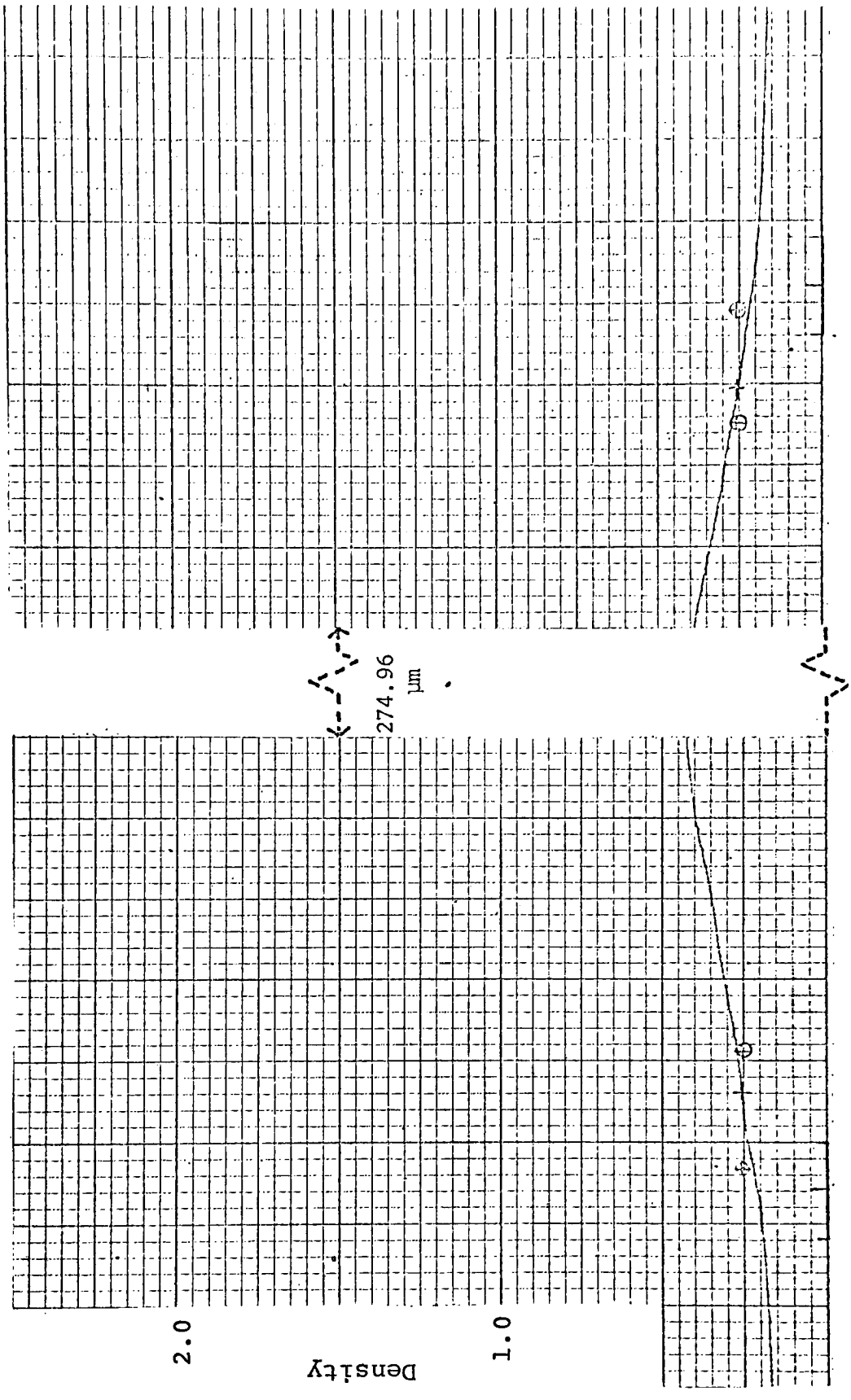

FIGURE 21. Microdensitometer Trace of 295.3 Micrometer
Wide Image, 0.45 Density Maximum

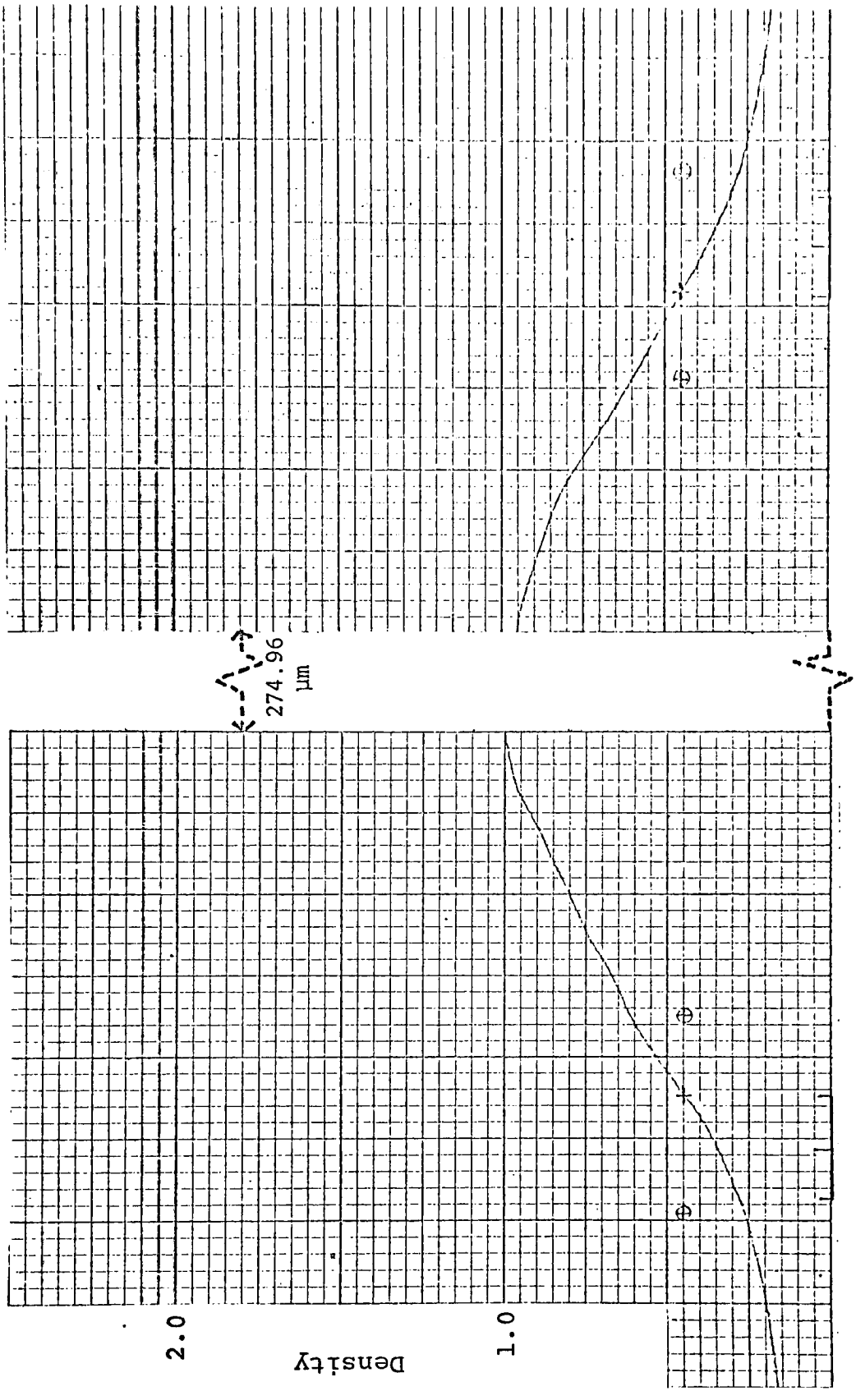

Distance 1 square = 0.4166 micrometer

FIGURE 22. Microdensitometer Trace of 295.3 Micrometer Wide Image, 1.41 Density Maximum

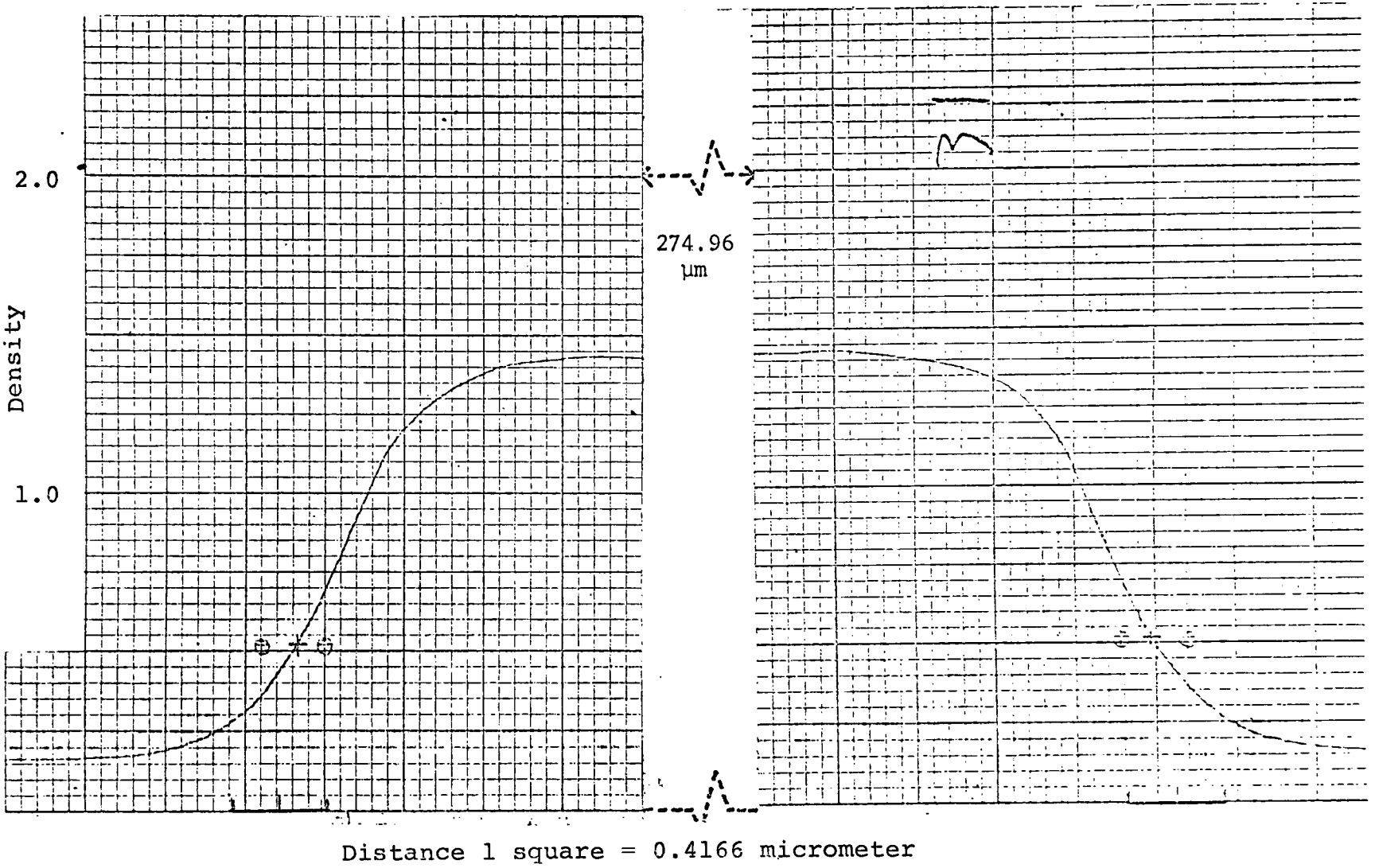

FIGURE 23. Microdensitometer Trace of 295.3 Micrometer Wide Image, 1.41 Density Maximum

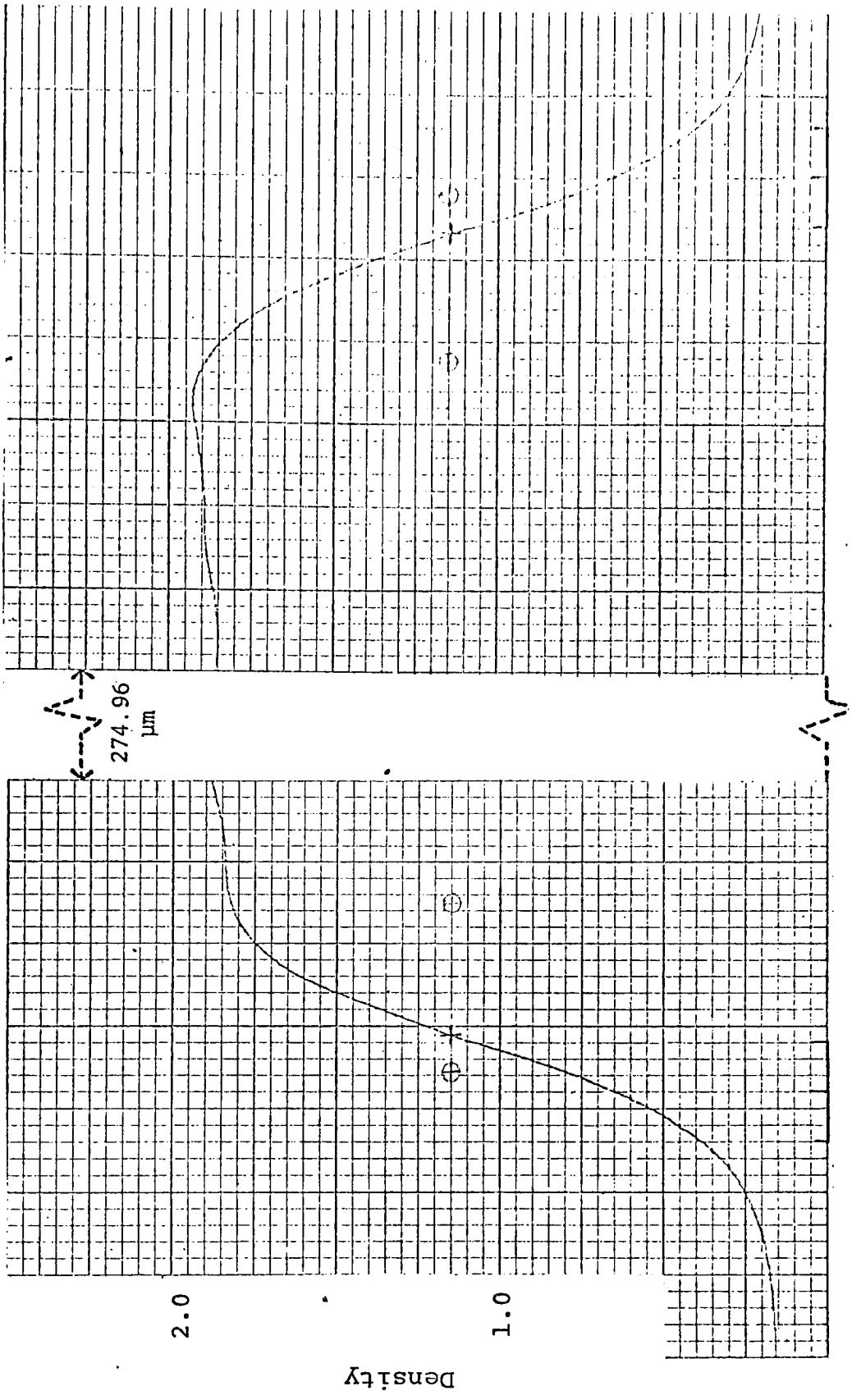

FIGURE 24. Microdensitometer Trace of 295.3 Micrometer Wide Image, 1.90 Density Maximum

Distance 1 square = 0.4166 micrometer

Visual Display of Measurement Error

Figure 25 is a plot of mean measurement error in percent as a function of image width for each image density. The data is averaged over ten samples, five operators with two replicates. This figure also displays the potential interaction of image width and image density as they affect mean measurement error. Because the lines frequently cross in Figure 25, one would expect a significant interaction between image width and image density. The rigorous statistical analysis of variance confirms that the interaction between image width and image density is significant to measurement error.

Figure 26 is a plot of mean measurement error as a function of image width for each operator. The data is averaged over eight samples, four densities with two replicates. This figure also displays the potential interaction of image width and operators as they affect mean measurement error. Because the lines look generally parallel in Figure 26 (except for Operator 1 measuring the 6.9 micrometer wide image), one would not expect a significant interaction between image width and operators. The rigorous statistical analysis of variance confirms this result.

Figures 25 and 26 graphically illustrate a relationship between measurement error and image width. The edge pointing errors analyzed in this experiment are significant (in terms of percent error) for images up to about 75 micrometers in

width. No consistent relationship between density and measurement error can be detected, and, in fact, the rigorous statistical analysis shows density to be not significant in this experiment.

None of the operators appears to be consistently in error, although operator 1 deviates in his measurement of the 6.9 micrometer wide image.

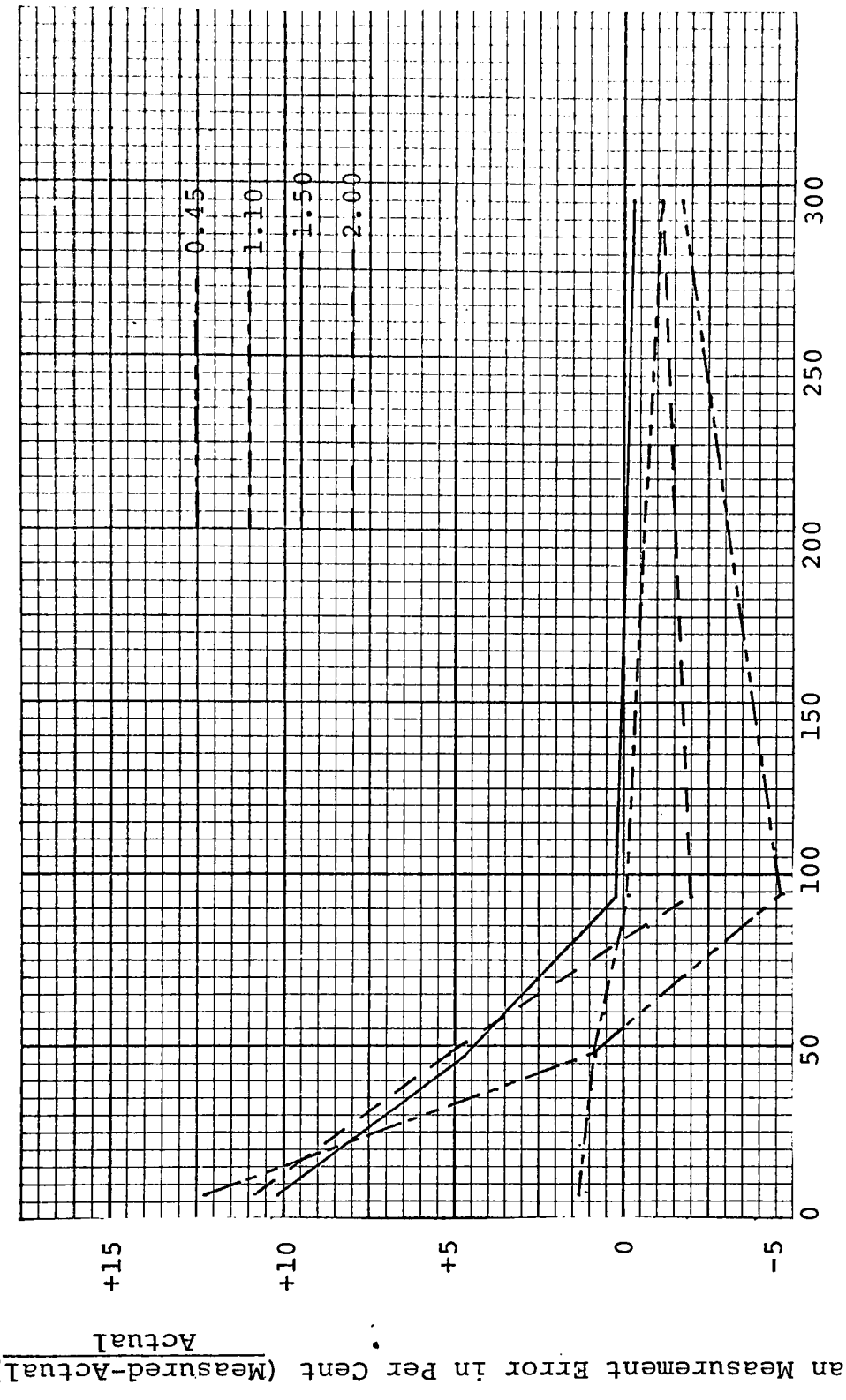

Figure 25. Mean Measurement Error as a Function of Image Width for Each Image Density

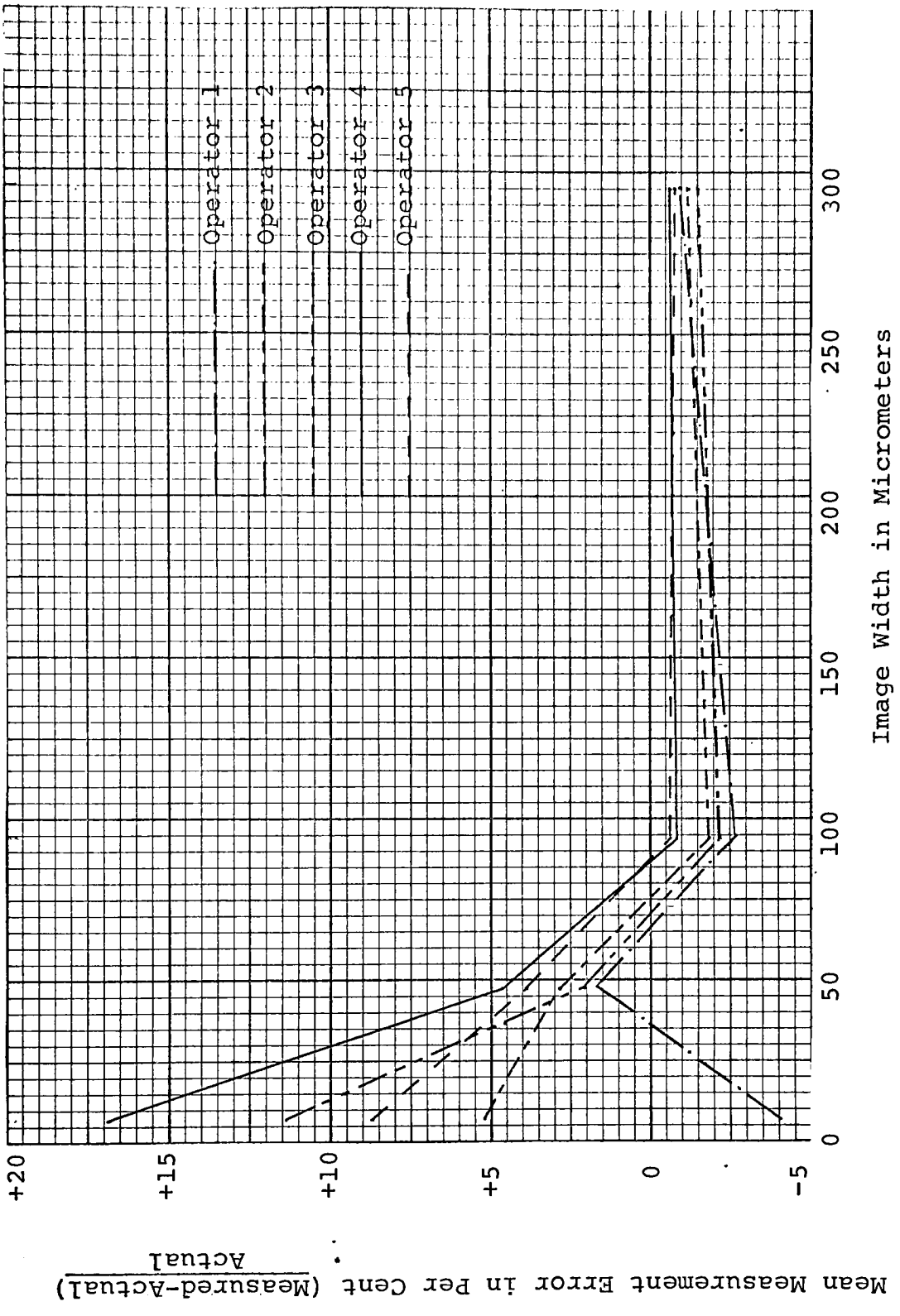

Figure 26. Mean Measurement Error as a Function of Image Width for Each Operator

DISCUSSION OF RESULTS

The rigorous statistical analysis of the experiment clearly shows that measurement error is dependent upon which operator was taking the measurement. In fact, the ranges of the ten individual measurements of the same image by five operators were surprisingly high. The largest range of error was 11.5 micrometers over approximately a 300 micrometer image (see Figure 22). For the smallest image of 6.9 micrometers, the range of error was such that an individual measurement could be in error in pointing by as much as 30 percent. The range of ten individual measurements could be as high as 65 percent of the true dimension. However, the mean of the ten measurements was never more than twelve percent in error (0.8 micrometer) for the 6.9 micrometer image. This result means that for the individual event of one operator using one instrument to make one measurement the answer could be grossly in error. For critical measurements, more than one operator should be used, and each operator should repeat his measurement more than once. The exact number of operators and replicates should be determined for the particular individual measuring conditions through statistical experimentation.

Measurement error in this experiment was significantly dependent upon the width of the image. Theory indicates that this would be expected in that each of the elementary

spread functions throughout the width of the image would have some contribution, however slight, to the spread at the edge of the image (see Figure 3). However, the magnitude of the measurement error as a function of image width appears higher than what might be expected theoretically. The variance of the mean measurement error due to the factor "image width" in the experiment is not only dependent upon the operator pointing error, but on the experimental determination of the aerial image width. This is true since measurement error is the difference between the measured width and the experimentally determined aerial image width. The determination of aerial image width is described in a previous section. The techniques, although newly developed for the experiment, were sound, and no flaw can be detected in the experimentation. The measurement error as a function of image width is considered to be satisfactory for this experiment, but this function should not be extrapolated to any general applications. Much more data must be collected for this result to be verified beyond this limited test.

Density was not a significant factor at the .01 level in the statistical analysis of this experiment. Theory predicts that in fact, the image does widen in the emulsion with increasing exposure. The Theoretical Background of this paper cites several historical references proving the phenomenon of turbidity or spread function and its dependence on exposure. Two reasons exist for not finding

significance for the factor density. The first would be that the experiment is not sensitive enough to detect the difference. The expected mean squares in the statistical analysis of variance dictate that the factor density be tested against the density and width interaction term. The interaction term was highly significant and this tended to dilute the test of significance for density. It is worth noting that density would have been significant in a test where $\alpha=.10$. Even in the analysis of variance shown in Table 10, density cannot be ignored because the density and width interaction term is significant. This means that care must be taken as to which width we are measuring at which density since there is not a linear functional relationship between the two when considering measurement error. The second reason for non-significance for the factor density is that the operators may have been compensating in some psychophysical way for the image widening at the higher densities. The operators in fact did not consistently select the same density level on the slopes of the edges. As the exposure increased for aerial images of the same width, the operators generally chose higher densities in their selection of the edge of the image. If a constant density level were chosen to determine the image width in Figures 9-24, the images consistently widen as exposure is increased for each of the four original targets. The width at the half amplitude of the edge is much more reliable in this experiment in

determining the trace aerial image width than is a constant density point. An approximation for determining the density at half amplitude is $D_{1/2}=D_{min}+(\frac{Dmax-Dmin}{2})$. A visual examination of Figures 9-24 reveals that $D_{1/2}$ and the average of ten measurements are nearly equal in their overall ability to determine the width of the aerial image.

Figures 9-24 demonstrate visually the conclusions drawn in the Analysis of Variance. They confirm that the average of ten measurements can be expected to be closer to the true width than any individual measurement. The graphs demonstrate, as do Figures 25 and 26, that for larger image widths the operators tended to underestimate the true aerial image width. The two most serious errors in underestimation occurred with the lowest contrast image of the 100 and 300 micrometer image. Intuitively, these would be the two most difficult images to measure. The measurements of the highest contrast image of the 100 and 300 micrometer image resulted in underestimation of image width. This could be due to previous training of instrument operators to visually compensate for the spreading of dark images on a light background. The microcamera imaging process used in this experiment may not have introduced as much image spread as normally encountered in the day-to-day experience of instrument operators.

The experimental results indicate that a more objective method than visual selection of edges for image measurement

must be developed. Increased training of operators and the statistical use of more operators may be a solution. Automated edge selection is shown in the experiment to be as accurate as the average of ten visual measurements, and automated techniques have the potential for being faster and less expensive.

CONCLUSIONS

An evaluation of data and results produces the following conclusions:

1. Operators, Image Width, and the interaction of image width and image density are significant factors in the visual measurement of microimages.

2. A consistent relationship between density and measurement error was not found. In fact, the rigorous statistical analysis indicates that density is not significant in this experiment.

3. The edge pointing errors analyzed in this experiment are significant (in terms of per cent error) for images up to about 75 micrometers in width.

4. The system can be calibrated; i.e., through careful experimental design and statistical techniques, the sources of mensuration error can be isolated. Follow-on

steps can be taken to eliminate each individual source of error. The errors within and among operators appear to be the largest source of error and efforts must be made to reduce this source. Operator training or automated techniques would be an acceptable solution. The image spread within the emulsion is another significant source of error. An image formation math model could reduce the error from this source.

5. The microdensitometer can be used as a precise mensuration device. Positional data was accurate from the device. Densitometric data (as a function of position) proved to be as accurate for mensuration as was the average of ten operator measurements.

BIBLIOGRAPHY

Allendoerfer, C. B. and Oakley, C. O. Principles of Mathematics. New York: McGraw Hill Book Co., (1955).

Altman, J. H. "Photography of Fine Slits Near the Diffrac-Limit," Photographic Science and Engineering. Vol. 10, 140 (1966).

Breido, I. I. Soviet Astronomy AJ. Vol. 2, 589 (1968).

Charman, W. N. "Visual Factors in Size Measurement by Microscopy". Optica Acta. Vol. 10, 129 (1963).

Eastman Kodak Company. Techniques of Microphotography. Rochester, N.Y.: (1967).

Goldberg, E. "On the Resolving Power of the Photographic Plate". Photographic Journal (Royal Photographic Society Journal).

Hendriksen, Soren W. "Camera Design for Photography of Artificial Satellites". Photographic Science and Engineering. Vol. 6, 318 (1962).

James, T. J. and Higgins, G. C. Fundamentals of Photographic Theory. Hastings on Hudson, New York: Morgan and Morgan Inc., 1968.

Levy, Marilyn. "The Sensitometric Characteristics of Micro-images". Photographic Science and Engineering. Vol. 6, 307 (1962).

Mees, C. E. K. and James, T. H. The Theory of the Photographic Process 3rd edition. New York: The Macmillan Co., (1966).

Rickmers, A. D. and Todd, H. N. Statistics, An Introduction. New York: McGraw Hill Book Co., (1967).

Ross, F. E. The Physics of the Developed Photographic Image. New York: D. Van Nostrand Company, (1924).

Smith, W. J. Modern Optical Engineering. New York: McGraw Hill Book Co., (1966).

Stevens, G. W. W. Microphotography. New York: John Wiley Co., (1967).

Thompson, M. M. editor. Manual of Photogrammetry. Falls Church, Va.: American Society of Photogrammetry (1966).

Todd, H. N. and Rickmers, A. D. Image Technology. Vol. 11, 55 (1969).

Tregillus, L. W. "Image Characteristics in Kodak Bimat Transfer Film Processing". Journal of Photographic Science. Vol. 15, 129.

APPENDIX - THE STATISTICS

The experiment was designed, conducted, and analyzed on a statistical basis using a three factor, crossed experimental design with mixed levels. An analysis of variance was performed for the test of significance with a confidence level of 99 percent. The three factors were arranged as follows:

Factor	Symbol	Number of Levels	Approximate Value of Levels
Operators	O	5	not applicable (qualitative)
Image Width	W	4	10, 40, 100, 300 μm
Image Density	D	4	.5, 1.0, 1.5, 2.0

The basic mathematical model for the statistical analysis of this experiment is:

$$X_{ijkl} = u+O_i+W_j+D_k+O_iW_j+O_iD_k+W_jD_k + e_l(_{ijk})$$

X_{ijkl} = a response variable - measurement error

u = general level of the response

O_i, W_j, D_k = effect due to Operators, Image Width, Image Density

O_iW_j = effect due to interaction of Operators and Image Width

O_iD_k = effect due to interaction of Operators and Image Density

W_jD_k = effect due to interaction of Image Width and Image Density

$O_iW_jD_k$ = effect due to interaction of Operators, Image Width and Image Density

$e_1(_{ijk})$ = experimental error

This experiment is designed to answer the following questions with 99 percent confidence:

1. Is there a significant difference in measurement error when different operators are used for the experiment?
2. Is there a significant difference in measurement error when different image widths are used in the experiment?
3. Is there a significant difference in measurement error when different image densities are used in the experiment?
4. Is there a significant interaction between operators and image width?
5. Is there a significant interaction between operators and image density?
6. Is there a significant interaction between image width and image density?
7. Is there a significant interaction between operators, image width, and image density?

The table of treatment combinations is shown in Table 9 in

the section on Statistical Analysis. Random and fixed factors are given in Table 12. The table of expected mean squares is shown in Table 13.

TABLE 12. Factors, Random or Fixed

Factor	Random or Fixed
Operators	Fixed
Density	Random
Width	Random

TABLE 13. Expected Mean Squares

	Fixed i,5	Random j,4	Random k,4	Random l,2	EMS
O_i	0	4	4	2	$32\sigma_i^2+8\sigma_{ij}^2+8\sigma_{ik}^2+2\sigma_{ijk}^2+\sigma_e^2$
D_j	5	1	4	2	$40\sigma_j^2+10\sigma_{jk}^2+\sigma_e^2$
W_k	5	4	1	2	$40\sigma_k^2+10\sigma_{jk}^2+\sigma_e^2$
OD_{ij}	0	1	4	2	$8\sigma_{ij}^2+2\sigma_{ijk}^2+\sigma_e^2$
OW_{ik}	0	4	1	2	$8\sigma_{ik}^2+2\sigma_{ijk}^2+\sigma_e^2$
DW_{jk}	5	1	1	2	$10\sigma_{jk}^2+\sigma_e^2$
ODW_{ijk}	0	1	1	2	$2\sigma_{ijk}^2+\sigma_e^2$
$E_{l(ijk)}$	1	1	1	1	σ_e^2

The following tables of numbers indicate the basic arithmetic performed in arriving at the statistical results. The arithmetic was performed both by computer and completely recalculated manually. The hand evaluations are shown. Using Table 9 - Treatment Combinations, each factor was first summed over, as shown in Tables 14 - 16.

TABLE 14. Summed Over Factor - Width

	DENSITY				
OPERATOR	.41	1.00	1.40	1.90	TOTAL
1	-26.7	-9.7	+0.2	-2.7	-38.9
2	-13.7	-7.7	+1.3	-17.2	-37.3
3	-19.7	-5.7	+3.8	-4.7	-28.3
4	-6.7	+9.3	+8.3	+2.3	+13.2
5	-16.2	-3.2	+9.3	+3.8	-6.3
TOTAL	-83.0	-19.0	+22.9	-18.5	-97.6

TABLE 15. Summed Over Factor - Operator

	DENSITY				
WIDTH	.41	1.00	1.40	1.90	TOTAL
6.9	+5.5	+1.0	+7.0	+7.5	+21.0
48.7	+4.5	+4.5	+23.9	+25.0	+57.9
94.7	-44.0	-0.5	+1.5	-18.5	-61.5
295.3	-49.0	-24.0	-19.5	-32.5	-115.0
TOTAL	-83.0	-19.0	+22.9	-18.5	-97.6

TABLE 16. Summed Over Factor - Density

	WIDTH				
OPERATOR	6.9	48.7	94.7	295.3	TOTAL
1	-2.2	+6.3	-19.1	-23.9	-38.9
2	+6.3	+7.9	-17.1	-34.4	-37.3
3	+2.8	+10.9	-14.1	-27.9	-28.3
4	+9.3	+17.9	-5.6	-8.4	+13.2
5	+4.8	+14.9	-5.6	-20.4	-6.3
TOTAL	+21.0	+57.9	-61.5	-115.0	-97.6

The Sums of Squares for the ANOVA table were determined as follows:

$$SS\ (Total) = \Sigma\ (X_{ijk})^2 - (T...)^2$$

n = number of observations = 160

T... = sum over all observations

SS (Total) = 1097.30 - 59.54 = 1037.76

SS (Operator= $\frac{1}{32}[(38.9)^2+(37.3)^2+(28.3)^2+(13.2)^2+(6.3)^2]$-
59.54 = 62.95

SS (Width)= $\frac{1}{40}[(21.0)^2+(57.9)^2+(61.5)^2+(115.0)^2]$-59.54=460.49

SS (Density)= $\frac{1}{40}[(83.0)^2+(19.0)^2+(22.9)^2+(18.5)^2]$-59.54 =
143.39

SS (Operator X Density)=SS (Total-Table 13)-SS (Operator) -
SS (Density) =243.20-59.54-143.39=36.86

SS (Density X Width)=SS (Total-Table 14)-SS (Density) -
SS (Width) =718.21-143.39-460.49=114.33

SS (Operator X Width)=SS (Total-Table 15)-SS (Operator) -
SS (Width) =546.41-62.95-460.49=22.97

SS (Error) = 146.18

The ANOVA table can now be derived from the above data. The table is listed as Table 10 of this paper.